Dissertation

Submitted to the Combined Faculties for the Natural Sciences and for Mathematics
of the Ruperto-Carola University of Heidelberg, Germany
for the degree of Doctor of
Natural Sciences

Presented by M.Sc. Biotech. Luca Guglielmi
born in: Mondovì, Italy

Oral examination:
March 2nd 2018

A Wif1 mediated feedback loop suppresses premature Wnt signaling in nascent habenular neurons

Referees: Prof. Dr. Joachim Wittbrodt

PD. Dr. Matthias Carl

Table of contents

Summary

Precise temporal and spatial control of cell signaling processes is pivotal for embryonic development. A vast number of secreted signaling molecules such as Wnt ligands travel between cells and tissues and influence their fate. If they are to induce a signaling cascade depends on various control mechanisms of potential target cells. These can include the temporal expression control of pathway components or the generation of signaling agonisers or antagonisers. Control of Wnt/beta-catenin signaling is important for the establishment of left- rigt (l-r) neuronal asymmetries of the evolutionarily conserved habenulae in the vertebrate dorsal diencephalon. During neurogenesis, this pathway is activated only when habenular precursor cells become post-mitotic, although Wnt ligands secreted by the adjacent mid-diencephalic organizer (MDO) surround these cells much earlier. The underlying control mechanism and its purpose have remained unexplored. We find that Wnt signaling is indeed initially inhibited in habenular precursors and that this is required for habenular neurons to subsequently adopt different neuronal fates. Indeed, premature induction of the pathway critically delays neuronal differentiation which ultimately lead to precursor differentiation into only one out of two neuron types of the habenulae on both sides of the brain. We further show that the early activation of Wnt signaling is naturally prevented by Wnt inhibitor factor 1 (Wif1), which is specifically expressed in the habenulae until precursors become post-mitotic. Suppression of *wif1* phenocopies the effect of early Wnt induction. Furthermore, *wif1* expression is positively regulated by Wnt signaling showing that *wif1* is functioning within a negative feedback loop. Our data are consistent with a model by which Wif1 dynamically shields early multipotent habenular precursor cells from incoming Wnt ligands secreted by the MDO and possibly other the sources until they become post-mitotic and differentiate into neurons. *wif1* and different Wnt ligands are overlappingly expressed in a number of developing structures including both the habenulae the downstream target the interpenduncular nucleus (IPN). This suggests that the Wnt/Wif1 buffering system may serve as a general mechanism for temporally tuning neurogenesis across the different nuclei of the brain.

Zusammenfassung

Eine genau abgestimmte zeitliche und räumliche Kontrolle von Zellsignalprozessen ist für die Embryonalentwicklung ausschlaggebend. Dabei bewegen sich eine große Anzahl an sekretierten Signalmolekülen wie zum Beispiel Wnt Liganden zwischen Zellen und Geweben und beeinflussen deren Schicksal. Ob diese Signalmoleküle eine Signalkaskade in Gang setzen, hängt von verschiedenen Kontrollmechanismen der potentiellen Zielzellen ab, welche die zeitlich kontrollierte Expression von Signalwegkomponenten oder die Generierung von Signal Agonisten und Antagonisten beinhalten können. Die Kontrolle der Wnt/beta-Catenin-Signalgebung ist für die neuronale Diversität der evolutionär konservierten Habenulae im dorsalen Dienzephalon der Wirbeltiere notwendig. Im Laufe der Neurogenese wird dieser Signalweg aber erst in den post-mitotischen Habenular-Vorläuferzellen aktiviert, obwohl Wnt-Liganden aus dem benachbarten mid-dienzephalen Organisator (MDO) diese Zellen schon viel früher umgeben. Der zugrundeliegende Kontrollmechanismus und Zweck blieben bisher noch unerforscht. Wir zeigen, dass die Wnt-Signalgebung in der Tat zunächst in den habenularen Vorläuferzellen gehemmt wird, was erforderlich ist, damit sie sich später nicht nur zu einem Nervenzelltyp sondern zu verschiedenen entwickeln können. Diese Hemmung wird durch den sekretierten Wnt-Inhibitionsfaktor 1 (Wif1) vermittelt, der seinerseits durch Wnt-Signalgebung positiv reguliert wird. Demnach stimmen unsere Daten mit einem Modell überein, in welchem Wif1 die frühen multipotenten habenularen Vorläuferzellen mittels eines dynamischen Puffersystems solange gegen Wnt-Liganden aus der MDO oder möglichen anderen Quellen abschirmt, bis sie post-mitotisch werden und zu Nervenzellen differenzieren. Die überlappende Expression von Wif1 und Wnt Liganden in mehreren Bereichen des Gehirns könnte auf einen generellen Mechanismus zur zeitlichen Kontrolle der Nervenzellentwiclung schliessen.

1.Introduction

1.1 Structural and functional brain asymmetries

During evolution, vertebrates have developed an impressive variety of complex behaviors. This was likely possible due to the natural selection of fruitful neuronal strategies which became inscribed within the architecture and the functioning of the brain. Left-Right (l-r) brain asymmetries are traces of this evolutionary heritage and to decipher their biological role is still a major challenge in modern neuroscience. In humans, left right differences in the anatomy of the brain can be observed at different levels (Concha et al., 2012, Güntürkün and Ocklenburg 2017). Grossly, the right hemisphere can be distinguished from the left by observing the size and shape of brain areas (Arthur W. Toga & Paul M. Thompson, 2003), like the Broca's area which is markedly larger on the left (Schenker et al., 2010; Rilling, 2014). On a microstructural level, differences in circuit architectures are observed in for instance the auditory and language cortex, where the organization of the cortical columns on the left hemisphere differ from the corresponding regions on the right (Hutsler and Galuske, 2003, Güntürkün and Ocklenburg 2017). Finally, l-r differences are also found in gene expression patterns. This is true for the language cortex where neuron specific genes are differentially expressed across the left and the right side of the brain (Karlebach and Francks, 2015). Interestingly, hemispheric asymmetries extend also to the way the human brain is functioning (Concha et al.,2012; Duboc et al., 2015 Güntürkün and Ocklenburg 2017). Indeed, functional neuroimaging approaches have revealed how for instance the language system (Corbalis. 2015), processing of visual and auditory stimuli (Vogel et al., 2003; Tervaniemi and Hugdahl, 2003) and even emotional processing (Grimashaw and Carmel, 2014) are markedly lateralized. Therefore, hemispsheric asymmetries seem to be frequently involved in human brain architecture and function (Güntürkün and Ocklenburg 2017), however their impact on brain processing and cognition is still poorly understood (Bianco et al., 2008; Concha et al.,2012, Güntürkün and Ocklenburg 2017). Recent studies of the brain of different vertebrates begin to shed light on this fascinating mechanism, significantly increasing our knowledge on the genetic and neuronal bases underlying structural and functional brain lateralization.

1.2 Brain asymmetries are widespread in the animal kingdom

Left-right asymmetries are a highly conserved feature of the animal brain as they can be observed in species which are phylogenetically very distant (Concha et al., 2012; Güntürkün and Ocklenburg 2017). For instance, In the nervous system of the nematodes *caenorabditis elegans* l-r asymmetries can be observed in both AWC and ASE sensory systems, which are required for odor and taste perception respectively (Hobert et al., 2002). Both these sensory system consist of a set of two neurons, one on the right (AWC-R/ASE-R) and on the left (AWC-L/ASE-L). In the olfactory system, the expression of the *str-2* encoded olfactory receptor is stocastically turned off in one of the two AWC neurons, this in turn enables proper odor discrimination and chemiotaxis. Similarly, in the ASE system, ASE-L expresses a different set of sensory receptor of the guanilil cyclase class (Gcy) compared to ASE-R, this difference in receptor distribution is conferring the ability to sense a broader spectrum of water soluble compounds (Wes and Bargmann., 2001; Hobert et al., 2002; Ortiz et al., 2009; Güntürkün and Ocklenburg 2017). In Chick, well known neuronal symmetries exist at the level of the visual system (Rogers et al., 1988; Koshiba et al., 2003). During embryonic development, only the right eye is accessible to light due to the positioning of the embryo within the egg. As a consequence, the visual thalamus (lateral geniculate nucleus, LGN) on the right side, will develop more thalamofungal projections toward the ipsilateral and contralateral iperpallium compared to the right thalamus (Rogers et a., 1999; Koshiba et al., 2002; Koshiba et al., 2003). This is correlated with the lateralized use of the eyes during the post-embrionic life (Dharmaretran et al., 2005): The right eye will specialize in the resolution of smaller objects, like grains on a background of pebbles. The left eye will be used for sensing macroscopic environmental changes like the overhead approaching of a predator (Rogers et al., 2000; Rogers et al., 2007; Concha et al., 2012). These are just few examples of the numerous strategies nature used to shape laterality in the animal brain (Concha et al., 2012; Güntürkün and Ocklenburg 2017). The best described neuroanatomical asymmetries to date are situated within the habenular circuit in the zebrafish epithalamus and are represented as l-r difference in habenular circuit sub-nuclear composition and connectivity pattern (Gamse. et al., 2003; Aizawa. et al.,

2005; Bianco. et al., 2008). Indeed, thanks to its suitability for imaging approaches and genetic manipulation, the zebrafish model enables the fine dissection of genetic and the functional pathways which underlies the establishment of structural and functional asymmetires in the brain.

1.3 The habenular circuit in the zebrafish epithalamus

The Habenular circuit is part of the dorsal diencephalic conduction system (DDC), relaying information from the medial forebrain into mid- and hindbrain structures (Sutherland, 1982; Morgane et al., 2005; Bianco and Wilson 2009). In mammals, the habenular complex can be anatomically subdivided in two separate nuclei on each side of the brain: the medial (MHb) and lateral (LHb) habenulae (Herkenham & Nauta 1977; Bianco and Wilson, 2009; Beretta et al., 2012). These nuclei are physiologically involved in processing reward prediction and modulate behavioral responses toward adversive stimuli (Benabid & Jeaugey 1989, Bianco and Wilson 2009; Boulos et al., 2017). In the zebrafish embryonic brain, the habenular nuclei are composed of a ventral habenulae (vHb, which is homologous of the lateral habenulae in mammals) and a dorsal habenulae (dHb, which is homologous of the Medial habenulae) (Bianco and Wilson, 2009; Amo et al., 2010; Beretta et al., 2012; Beretta et al., 2013). The dHb nuclei can be grossly subdivided into two different neuronal populations, the medial habenular neurons (dHbm) and the lateral habenular neurons (dHbl) (Aizawa et al., 2005; Gamse et al., 2005; Aizawa et al., 2007; Bianco et al., 2008; Hüsken et al., 2014), which typically express different sets of potassium channel tetramerization domain containing genes transcripts (*Kctd2.1* for the dHbl and *kctd8* for the dHbm) (Aizawa et al., 2005; Gamse et al., 2005; deCarvalho et al., 2014) (Fig. 1A,C). Importantly, the size of these two neuronal population differ across the hemispheres. Namely, the dHbl population is larger on the left, whether the dHbm neuronal population is larger on the right (Aizawa et al., 2005; Carl et al., 2007; Bianco et a., 2008, Hüsken et al., 2014) (Fig.1 B,C). These different neurons project axons which segregate dorso-ventrally on their way to their midbrain target, the interpenduncular nucleus (Gamse et al., 2005; Bianco et al., 2008; Aizawa et al., 2005) (Fig. 1 A, B). dHbl neurons innervate the dorsal IPN (dIPN), which signals toward the

VTA (Ventral tegmental area) while dHbm neurons innervate the ventral IPN (vIPN) (Fig. 1B) which is connected to the median raphe (MR) (Aizawa et al., 2005; Yi-Chu et al., 2016). Interestingly, the habenular nuclei is also receiving lateralized afferent innervation from different sensory nuclei (Turner et al., 2016). On the left, the habenula is innervated by left positioned parapineal cells (Gamse et al., 2003; Garric et al., 2014; Turner et al., 2016) and receives excitatory monosynaptic inputs from bilateral EmT (eminentia thalami) in the thalamus (Turner et al., 2016; Concha et al.,2003; Zhang et al., 2017) (Figure B). Conversely, the right habenula is exclusively innervated by the mitral cells (MC) of the olfactory bulbs (OB) via the stria midullaris (Miyasaka et al., 2009; Gayoso et al., 2011; Krishnan et al., 2014; Turner et al., 2016). Therefore the left and the right habenulae receive lateralized innervation from

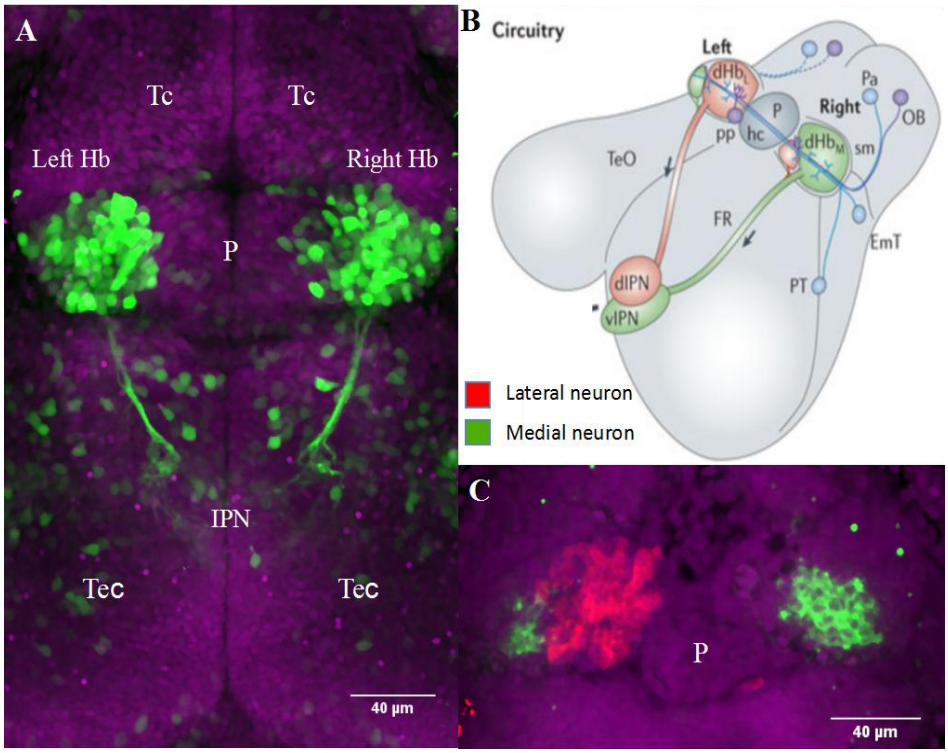

Figure 1:The asymmmetric habenular circuit

(A,C) Dorsal views, anterior to the top focused onto the dorsal diencephalon of (A) a reporter line marking habenular neurons and their projections with GFP (C) Differentialy labeled dHbl neurons (red) and dHbm neurons (green) at 3 dpf. Nuclei are DAPI labeled. (B) Adapded from Bianco et al., 2008: Representation of the zebrafish embryonic brain and the habenular circuit within. dHbm and dHbl neurons are differentially distributes and laterotopically innervate the IPN. Hb, habenula; IPN, interpeduncular nucleus; P, pineal gland; Tc, telencephalon; Tec, optic tectum; v,

upstream sensory nuclei and translate them along the dorso-ventral axes via laterotopic innervation of the IPN (Turner et al., 2016). This complex structural architecture has in turn, profound functional implications (see below).

1.4 Functional asymmetries in the habenulae

The habenular circuit in the Zebrafish is a particularly suitable for the study of brain lateralization as both functional and structural asymmetries are coexisting within the same circuit (Dreosti et al., 2014). The left and the right habenulae express different neurotransmitter genes, (Hong et al., 2013). The right habenula exclusively expressess choline acetyltransferase and vesicular acetylcholine transporter homologs genes (Hong et al., 2013) and optogenetic stimulation of the rHb elicit a tipical cholinergic response in IPN neurons likely mediated by α 2 and β4 acetilcholine receptors (Hong et al., 2013). The rdHb-vIPN colinergic pathway elaborates olfactive stimuly (Dreosti et al., 2014; Jetti et al., 2014) and its activation mediates avoidance behavior in response to adversive olfactive clues in a concentration dependent manner (Krishnan et al., 2014) (Fig. 2). in contrast, the left habenula expresses neuropeptides like *sst1.1* (somatostatin 1.1) and mediates the elaboration of visual stimuli (deCarvalho et al., 2014; Dreosti et al., 2014; Hüsken et al., 2014; Yi-Chu et al., 2016). The lHb indirectly receives visual information from the retinas via the EmT and its activation is required for the embryo to express light-preference behaviors (Zhang et al., 2017)(Fig. 2). Recent studies showed that both the left and right Hb are antagonistically active to regulate conflicts resolution and aggression. Indeed, increased activation of the lHb-dIPN-VTA correlates with a stronger predisposition to win. Conversely, activation of the rHb-vIPN-MR pathway correlates with an higher likelihood for the fish to lose (Yi-Chu et al., 2016) (Figure 2). Intriguingly, in manipulated brains in which the habenulae develop symmetrically displaying either a double left-or a double right phenotype it becomes responsiveless to either odour or

light respectively (Carl et al.,2007, Hüsken et al., 2014; Dreosti et al., 2014). Also, embryos developing symmetric habenulae display reduced exploratory behavior and increased cortisol levels, indicative of enhanced anxiety (Facchin et al., 2015). These findings are consistent with the idea that the establishment of consistent neuronal diversity in the habenulae is necessary for the Hb circuit to exert its multiple cognitive functions. This consistency, in turn, is generated as a result of a very dynamic interplay between different molecular players which act at different levels of the habenular neuron differentiation cascade.

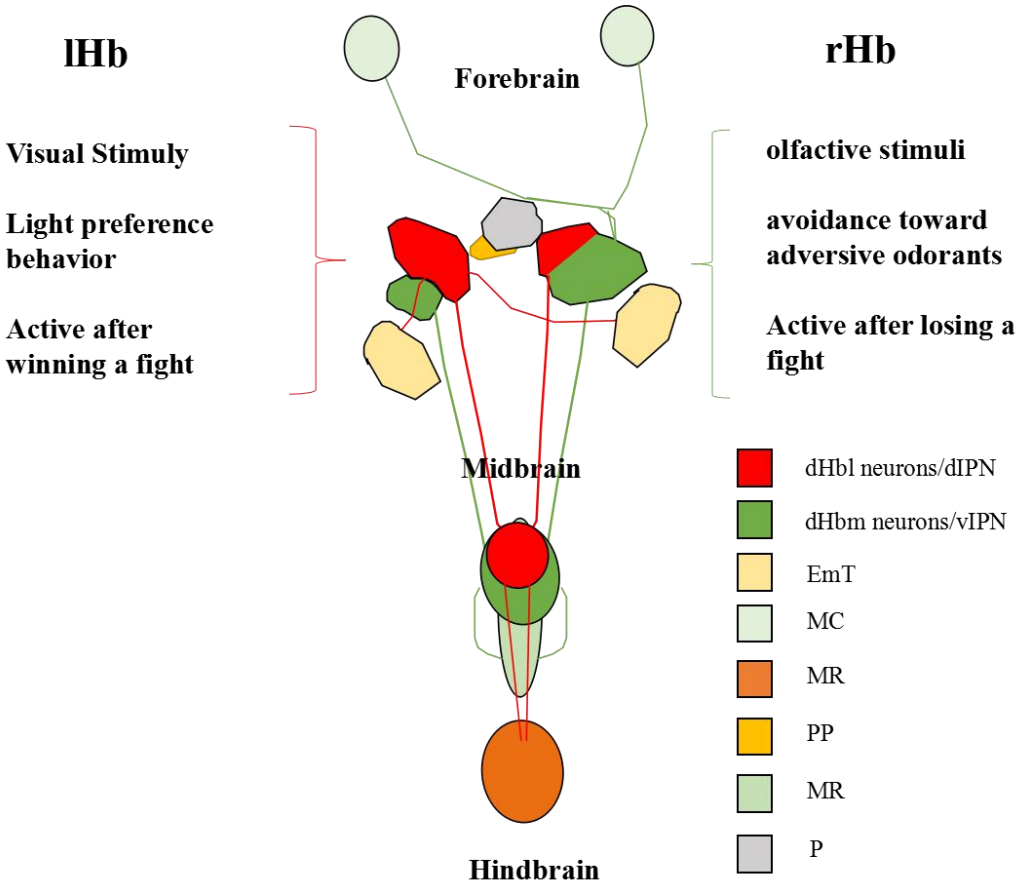

Figure 2: L-r asymmtries in habenular connectivity

Representation of afferent and efferent connectivity of the habenular circuit. The rHb relays information from the olfactory bulbs into the vIPN and MR. The lHb is innervated by both the EmT and the PP and project axons towrd the dIPN which is itself connected to the VTA. lHb, left habenulae; rHb, right habenulae; IPN, interpenduncular nucleus; d, dorsal; v, ventral; Emt, eminentia thalami; MC, median raphe; MC, mitral cells; PP, parapineal: P, pineal; VTA, ventral tegmental area.

1.5 The establishment of the habenular progenitor pool

Dorsal habenular neurons originates from a pool of stem cells in the dorsal diencephalon. These stem cells are located anterior to the pineal organ and they are dorsally positioned in respect to the Mid Diencephalic Organizer (MDO) (Scholpp et al., 2007, Hagemann and Scholpp, 2012; Cavodeassi and Houart, 2012), a signalling centre controlling regional differentiation of the neighbouring diencephalic areas (Scholpp et al., 2007). Before they differentiate into neurons, habenular precursors can be identified by the expression of two different markers, the homeodomain trascription factor *dbx1b* (Dean et al., 2014) and the chemokine (C–X–C motif) receptor 4b (*cxcr4b*) (Roussigné et al 2009). Dbx1 expression is firstly detected in between 20 and 24 hpf and marks precursors in active proliferation (Dean et al., 2014). Few hours later, around 30hpf, *cxcr4b* expression arises from a subset of *dbx1b* positive precursors and its expression is rapidly terminated as soon as dHb precursors become neurons around 36hpf (Roberson and halpern, 2017) (Dean et al., 2014; Roussigné et al., 2009; Halluin et al., 2016). This suggested that transitioning from dbx1b + progenitors toward cxcr4b+ cells may be indicative of the precursors exiting their proliferative phase and entering their neuronal lineage (Roberson and Halpern 2017). The MDO is a source of different morphogens like sonic hedgehog (Shh), Wnt signalling (Wnt) and Fibroblast grow factor signalling (Fgf) (Crossley et al., 1996; Hagemann and Scholpp, 2012; Mattes et al., 2012; Peukert et al., 2011; Picker et al., 1999; Cavodeassi and Houart, 2012). Shh signalling originating from the MDO has been proposed to have a pivotal role in the establishment of the habenular progenitor pool (Halluin et al., 2016; Roberson and Halpern , 2017). Indeed In *smoothened* mutants (*smo*$^{-/-}$), in which shh signalling is inactive, expression of both habenular precursors marker *dbx1b* and *cxcr4b* is strongly reduced. Precursor generation/maintenance seem to require persistent Shh signaling in between 16 and 24hpf as pharmacological inhibition of Shh at later staged does not affect the size of the Hb precursors population (Halluin et al., 2016). In addition to Shh also Wnt signaling seems to play a role in the establishment of the Hb precursor pool. Wntless (Wls) is a transmembrane protein required for the secretion of most Wnt lignds. In Wls mutants the size of both *dbx1b* and *cxcr4b* precursor population is reduced (Kuan

et al., 2005). However, the temporal requirement for Wnt signaling in this process is not known (Kuan et al., 2015)

1.6 Neurogenesis in the habenulae

Shortly after the establishment of the habenular progenitor pool around 20 hpf, these cells experience a phase of sustained proliferation (Aizawa et al., 2007; Dean et al., 2014). During this time, habenular precursors are equipotential, meaning that they have an equal likelihood to become dHbl or dHbm neurons (Aizawa et al., 2007) (Fig. 3A). Lineage restriction for these cells is firstly detected around 24 hpf, the time at which they undergo a first differentiation wave. This wave of differentiation is mainly influences on the left side and reaches its peak at 32 hpf (Fig. 3B). During this time, on the right side Hb precursor stay in an undifferentiated state. Shortly after the first differentiation wave, a second wave influencing mainly progenitor cells on the right, starting around 30 hpf and peaking at 48 hpf (Aizawa et al., 2007) (Fig. 3C). Notably, neurons born during the first differentiation wave have an higher likelihood to become dHbl neurons. In contrast, neurons born during the second differentiation wave become predominantly dHbm neurons (Aizawa et al., 2007) (Fig. 3B,C).Temporal regulation of this l-r difference in timing of neuron generation is controlled by Notch signalling pathway (Aizawa et al., 2007). Notch signalling is known to be an antagonizer of neurogenetic activity in neuronal stem cells and is often suppressed to enable neuronal fate specification. (Lovi and Artavanis-Tsakonas 2006; Huang et al., 2012). In embryos, in which Notch is ectopically up-regulated prior 30hpf, neurogenesis is delayed and dHbm are mainly generated on both side of the brain. Conversely, in embryos with inactive Notch signalling, premature differentiation result in the development of a double left habenula (Aizawa et al., 2007). This suggests that in between the first and the second differentiation wave the molecular environment within the epithalamus may be dynamically changing and in this way differentially affect the destiny of the neurons born at the time (Temple et al., 2001; Aizawa et al., 2007). However, the mechanism underlying the l-r differential activation of notch signalling is still unclear. Indeed both Notch ligands and effector genes are expressed symmetrically within the developing habenulae (Aizawa et al.,

2007), only exception is the notch downstream effector *her 6*, which is found to be slightly stronger on the right at 32 hpf (Aizawa et al., 2007). Therefore it is possible that additional mechanisms may either directly modulate Notch or act in parallel to ensure different timing of neurogenesis in the habenulae (Roussigné et al., 2009)

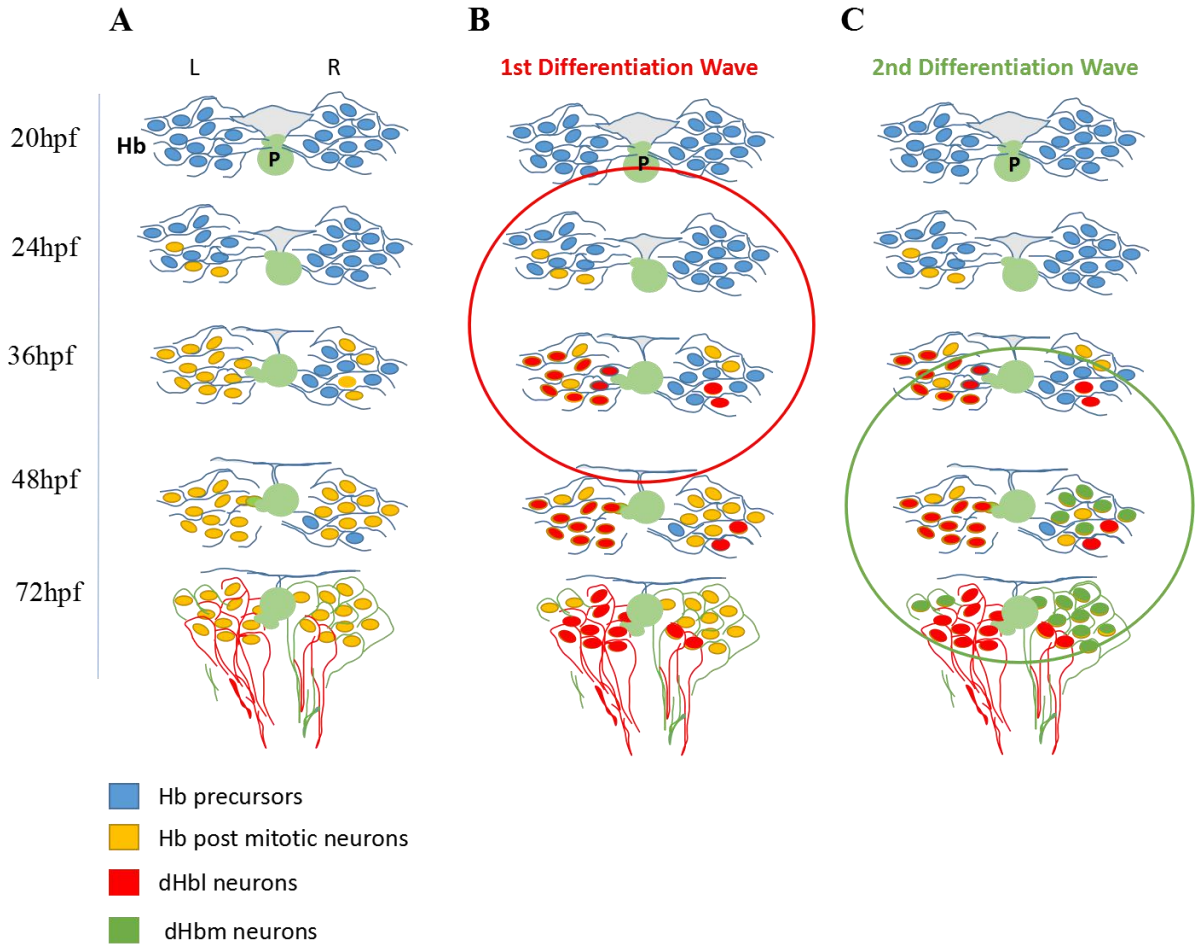

Figure 3: Asymmetric neurogenesis in the habenulae

Summary of events describing onset and progression of Hb neuron differentiation. (A) Neurogenesis occurs earlier on the left starting from around 24 hpf via two different differentiation waves. (B) During the first differentiation wave mainly dHbl neurons are generated. (C) During the second differentiation wave mainly neurons of the dHbm subtype are generated.

1.7 Symmetry breaking signals

Anatomical asymmetries in the epithalamus comprise the different left and right habenulae and the midline positioned Pineal Complex, which is itself composed of the pineal gland (P) and the parapineal nucleus (PP) (Concha et al., 2001). Importantly, on about the time Hb neurogenesis is starting on the left (24-30 hpf) PP cells detache from the anterior/medial region of the pineal and migrate toward the left (Concha et al., 2001). Later on, on about two days of development these cells will finally innervate the left habenulae (Turner et al., 2016). Ablation of PP cells prior 30hpf result in the habenulae to acquire a double right character by which mainly dHbm neurons are born on both sides of the brain (Concha et al., 2003) showing that the PP is required for left-differentiating Hb neurons to acquire the dHbl character (Gamse et al., 2003; Gamse et al., 2005). Parapineal cell migration depends on both Nodal sigalling and Fgf signalling (Concha et al., 2000; Concha et al., 2003; Regan et al., 2009). During development, Nodal signaling is classically involved in the establishment of the l-r body axis (Shier, 2003). Nodal gene expression in the left lateral plate mesoderm is known to establish the laterality of various organs like heart and pancreas (Hirokawa et al., 2006). In the brain, expression of Nodal genes can be detected in the epithalamus starting from 18hpf (Halpern et al., 2003). At this time the Nodal ligand *cylops* (Cyc), the Nodal secreted inhibitor *lefty-1* and the downstream transcription factor *pitx2* are selectively expressed on the left (Concha et al., 2000; Gamse et al., 2003 Rebagliati et al., 1998; Sampath et al, 1998; Regan et al., 2009). In embryos in which Nodal signalling is compromised neuroanathomical asymmetries still develop, however the laterality of both the PP nucleus and the Hb are randomized (Concha et al., 2000). While Nodal signalling is controlling directionality of parapineal migration Fgf signalling controls the migratory event per se (Regan et al., 2009). Indeed, In Fgf8 mutant *acerebellar* (*ace*) mutants the PP do not migrate and epithalamus develop symmetrically in the presence of left-sided Nodal signaling (Regan et al., 2009). Exogenous application of Fgf8 is capable to rescue the observed phenotype (Regan et al., 2009). Taken together, Nodal and Fgf signaling synergistically control PP cell migration on the left at about the same time when notch dependent neurogenesis is firstly occurring on the left. On top of these genetic interactions, the likelihood that habenular precursor will become one or the other

neuronal type is critically controlled by the levels of Wnt-Axin1-tcf7l2-beta- catenin signaling (Carl et al., 2007; Hüsken et al., 2014)

1.8 Wnt-Axin-1-Tcf7l2 signalling is required for habenular neuron to elaborate of the dHbm character

Canonical Wnt signalling is involved in the control of neuronal differentiation in both embryonic and post-embryonic brain (Carl et al., 2007; Wang et al., 2012). The activation of the pathway is archived via the binding of Wnt ligands to the Frizzled/LRP receptor complex which result in the recruitment of the β-catenin 'destruction complex' toward the membrane (MacDonald et al., 2009) (Fig. 4A). This complex is composed of cytosolic proteins like Axin-1, adenomatosis polyposis coli (APC), protein phosphatase 2A (PP2A), glycogen synthase kinase 3 beta (GSK3β) and casein kinase 1α (CK1α) and is normally inducing β-catenin degradation by targeting it for ubiquitination (MacDonald et al., 2009) (Fig. 4B). Therefore pathway activation result in β-catenin translocation into the nucleus where it binds to trascription factors of the Tcf family. Finally, the assembled trascriptional complex

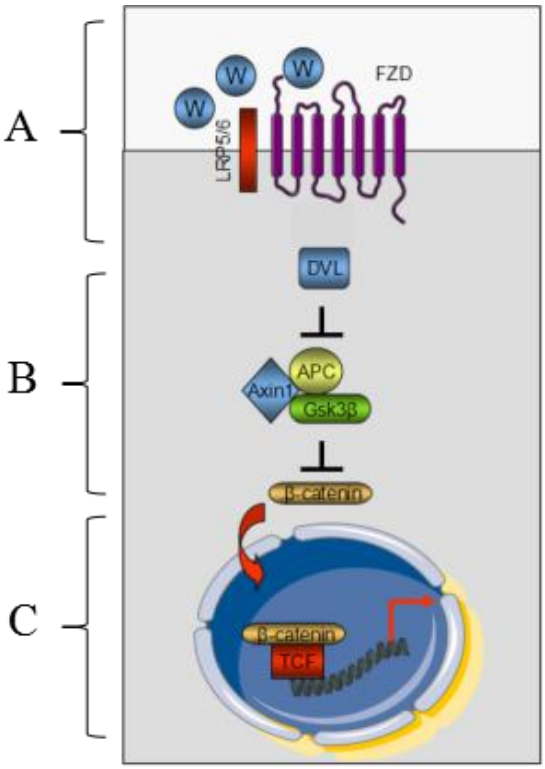

Figure 4:Canonical Wnt Signaling pathway

Schematic representation of the canonical Wnt signalling pathway. (A) Wnt ligands interact with the receptor complex FZD/LRP. (B) As a consequence of ligand binding, Dishevelled (DVL) is recruiting the β-catenin destruction complex toward the membrane. (C) β-catenin in then free to translocate into the nucleus where it bind to TCF transcription factor to induce the expression of Wnt downstream genes.

trigger the expression of Wnt- downstream genes (MacDonald et al., 2009) (Fig. 4C). In embryos mutant for *axin-1*, Wnt is constitutively up-regulated (Heisenberg et al., 2001; Carl et al., 2007). As a consequence, mutant embryos display reduced anterior brain structure like the thelencephalon and the eyes, while posterior areas like the diencephalon are markedly enlarged (Heisemberg et al., 2001; Carl et al., 2007). In these mutants, the habenulae develop symmetrically acquiring a double right character in which mainly dHbm neurons are born on both side of the brain and they symmetrically innervate the ventral IPN (Carl et al., 2007). Interestingly, the opposite phenothype is observed in mutants where Wnt signalling is suppressed. Embryos mutant for the transcriptional modulator *Tcf7l2* develop a symmetric habenulae with "double left character" where more dHbl are born on the right side and habenular projections target exclusively the dorsal IPN (Hüsken et al., 2014). This is phenocopied by parmacological inactivation of Wnt signaling between 35-36 hpf, showing that pathway activation is required within a very narrow time window (Hüsken et al., 2014). Tcf7l2 is found in post-mitotic neurons and its expression recapitulates dHb neuron differentiation starting first on the left side (Hüsken et al., 2014). Furthermore, transplantation experiments indicate that Tcf7l2 acts

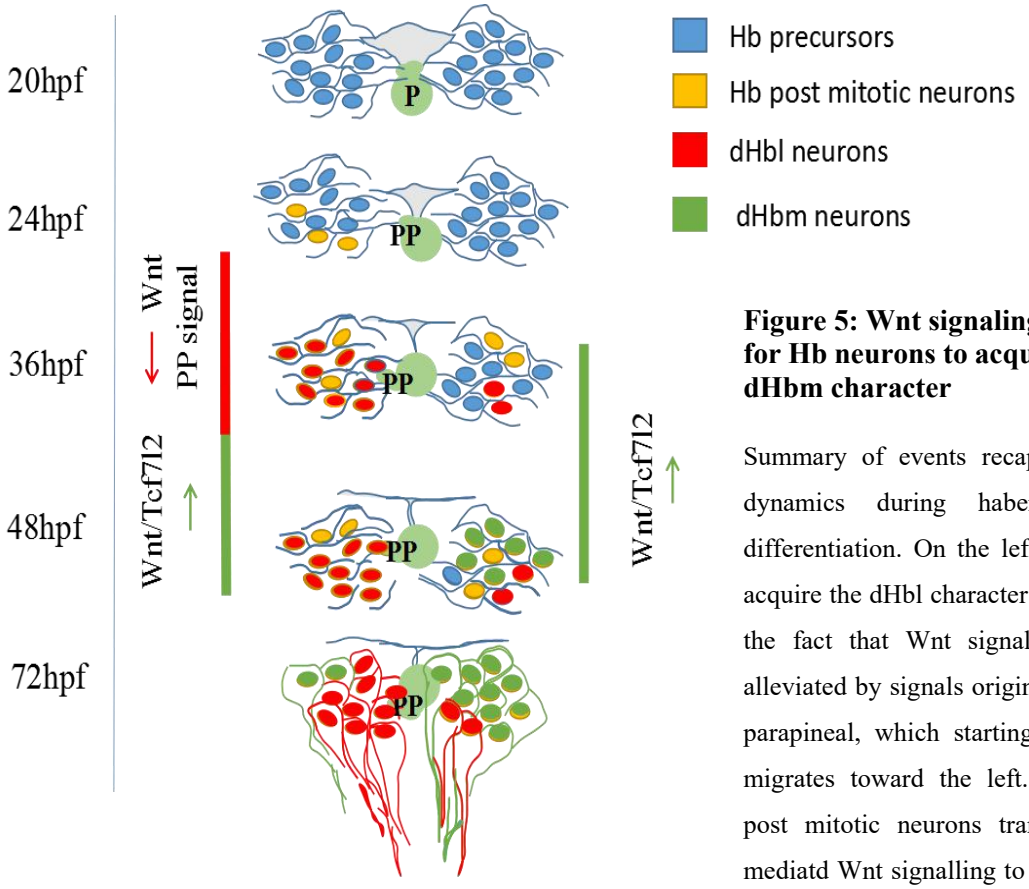

Figure 5: Wnt signaling is required for Hb neurons to acquire the dHbm character

Summary of events recapitulating Wnt dynamics during habenular neuron differentiation. On the left dHb neurons acquire the dHbl character. This is due to the fact that Wnt signaling is locally alleviated by signals originating from the parapineal, which starting from 24 hpf migrates toward the left. On the right post mitotic neurons transduce Tcf7l2 mediatd Wnt signalling to finally acquire the dHbm character.

cell-autonomously to bias post mitotic neurons toward the dHbm fate and does so without affecting the Notch dependent timing of neurogenesis (Hüsken et al., 2014). Importantly, parapineal ablation in *tcf7l2* mutants still result in a double left character, suggesting that symmetric dHbl phenotype is epistatic to the effect of parapineal ablation (Hüsken et al., 2014). Taken together these evidences suggest a scenario in which Tcf7l2 mediated Wnt signalling biases the destiny of post-mitotic neurons toward the dHbm character. On the left, the parapineal locally alleviates Tcf7l2 mediated Wnt signaling and in this way, neurons born during the first differentiation wave will acquire the dHbl character (Hüsken et al., 2014) (Fig. 5).

2. Aim of the Thesis

The levels of Wnt signalling are critically controlling whether post mitotic habenular neurons will acquire the dHbl or the dHbm character (Carl et al., 2007; Hüsken et al., 2014). Neurons born earlier on the left will experience low levels of Wnt signalling due to the parapineal signal and become dHbl neurons (Hüsken et al., 2014). Conversely, neurons born during the second wave on the right will transduce Tcf7l2 mediated Wnt signalling and finally acquire dHbm character (Hüsken et al., 2014). In this way, temporally regulated asymmetric neurogenesis in conjunction with Wnt signaling results in the differentially represented dHbl and dHbm habenular neuron population across the hemispheres (Carl et al., 2007; Hüsken et al., 2014). Intriguingly, transient interference with Wnt/beta-catenin signaling using drug treatments or transgenic techniques narrowed down the temporal requirement for pathway activation and dHbm neuron generation on about 2 hours between 35-36 hpf (Hüsken et al., 2014). These findings were rather surprising as several component of the Wnt-signaling cascade as axins, trascription factors of the the Tcf family and Wnt ligands are expressed before this time at least at mRNA level (Carl et al., 2007; Hüsken et al., 2014; Thisse and Thisse, 2005; Thisse and Thisse, 2008; Young et al., 2002), suggesting that Wnt signaling may be involved in processes other than dHb neuron specification. One possibility is that the levels of Wnt signalling may be temporally controlled and suppressed in developing habenular precursors until 36 hpf. In order to explore this intriguing possibility the following points were assessed:

- Visualization of Wnt signalling activity in the epithalamus during Hb precursor maturation/differentiation.
- Explore the consequences of premature manipulation of Wnt signalling on habenular circuit development.
- Identification of the likely molecule antagonizing Wnt signaling during the early phases of Hb neuron differentiation
- Identification of the mechanism underlying tight temporal control of Wnt signaling.

We found that Wnt signalling is naturally suppressed in developing Habenular precursors. Premature induction of Wnt signalling critically delays Hb precursors differentiation. As a consequence, Hb neurons on both side of the brain develop with characteristics typical of dHbm neurons. We identified the molecule mediating this suppression being the Wnt inhibitor factor 1 (Wif1). Wif1 is expressed in early habenular precursors and temporally complements Tcf7l2 expression. Suppression of Wif1 phenocopies the effect of early Wnt activation on habenular neuron differentiation. Its expression is positively regulated by Wnt signalling showing that the steady state of early Wnt signaling is achieved via dynamic negative feedback loop. Our findings uncover a novel role for Wnt signalling in habenular neuron differentiation and define a scenario in which “early” inhibition and subsequent “late” activation of Wnt signalling is required for Hb precursors to properly enter and complete their differentiation program. For the first time, we discovered an in vivo role for a Wnt/Wif1 feedback mechanism in steering neurogensis, which will well apply to many other neuronal populations in the light of similar temporal/spatial expression pattern of Wif1 and Wnt ligands.

3. Results

3.1 Wnt signaling is suppressed in early habenular precursors

Multipotent Hb precursors are born into a very dynamic molecular environment. As they undergo maturation, these cells are instructed by the temporal and spatial interplay of the different signaling pathways to finally acquire their morphological and functional commitment. The Wnt signaling pathway is required for habenular neurons to acquire the dHbm Identity and therefore the typical left-right asymmetry in Hb structure and function (Carl et al., 2007; Hüsken et al., 2014). Transient interference with Wnt/beta-catenin signaling using drug treatments or transgenic techniques narrowed down the temporal requirement for pathway activation and

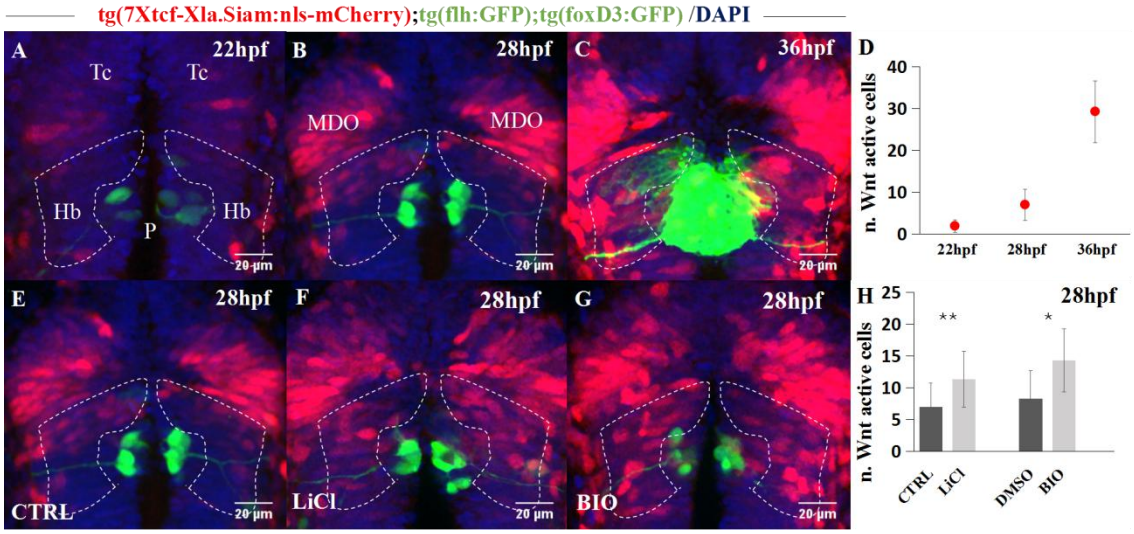

Figure 6: Wnt signaling activity in and around the developing habenulae.

(A-C, E-G) Dorsal views, anterior to the top focused onto the dorsal diencephalon of tg*(7xtcf-Xla.Siam:nlsmCherry); tg(flh:GFP); tg(foxD3:GFP)* transgenic embryos at stages indicated. DAPI stained nuclei are blue, red fluorescent nuclei indicate active Wnt signaling and the pineal complex is labeled in green for orientation. Dotted line encircles the region of the developing habenulae.(E) same as in B to enable comparison. (D) Graph shows the increasing number of Wnt active habenular precursors, which are (H) increased, when Wnt signaling was activated by drug treatments as indicated. Hb, habenulae; MDO, mid- diencephalic organizer; P, pineal; Tc, telencephalon.

dHbm neuron generation on about 2 hours between 35 and 36 hpf (Hüsken et al., 2014). These findings were rather intriguing indeed several component of the Wnt-signaling cascade as axins, trascription factors of the the Tcf family and Wnt ligands are expressed before this time at least at mRNA level (Hüsken et al., 2014), suggesting that Wnt signaling may be involved in processes other than dHb neuron specification. One possibility is that Wnt signaling may be suppressed in developing habenular precursor until 36 hpf. To support this hypothesis, we first assessed when Wnt activity is first detectable in the developing epithalamus by using Wnt read out line *tg(7xtcf-Xla.Siam:nlsmCherry)*^{ia5} (Moro et al., 2012). This transgenic line carries a monomeric Cherry protein (mCherry) under the control of seven multimerized TCF responsive elements upstream of the minimal promoter of the Xenopus direct β-catenin target gene *siamois* (Moro et al., 2012). By using this reporter we found that already from 22 hpf, few Wnt active cells are present in the presumptive habenula region (1, 9 +/- 1,5; n=11) (Fig. 6A,D) the number of which slightly increased by 28 hpf (7 +/- 3,73; n= 19) (Fig. 6B, D). At this time, cells of the anteriorly adjacent mid dyencephalic organizer (MDO) already show widespread Wnt activity. The number of fluorescent nuclei in the developing habenulae further increased by 36 hpf (29,3 +/-7; n=10) (Fig. 6C, D), suggesting Wnt activity in an increasing number of cells over time. These findings also indicate that Wnt signaling is normally not active in the majority of habenular precursors before 36 hpf. However, a few early habenular cells showed active Wnt signaling, which implies that possibly Wnt pathway components are readily present in all habenular precursors before 36 hpf, but that the pathway is normally suppressed. To assess this possibility, we activated Wnt signaling by blocking Gsk3β in *tg(7xtcf-Xla.Siam:nlsmCherry); tg(flh:GFP); tg (foxD3:GFP)* transgenic embryos for 30 minutes at 26 hpf using Lithium Chloride (LiCl) (Stambolic et al., 1996). In line with our theory, the treatment caused a significant increase of Wnt active habenular precursors at 28 hpf compared to the control (CTRL:7 +/- 3,73; n= 19; LiCl:11,35 +/- 4,4 ; $p < 0,003$; n= 17) (Fig. 6D, E). Similarly, treatments with the Gsk3β inhibitor (2'Z,3'E)-6-Bromo-indirubin-3'-oxime (BIO) (Meijer et al., 2003) caused an increase in the number of Wnt active cells compared with embryos treated only with DMSO (DMSO: 8,33 +/-4,32, n=6; BIO: 14,29 +/-4,96, n=7, p=0,04)(Fig. 6F) although the effect was less robust compared to LiCl treatments. These data allowed us to conclude that Wnt signalling is likely

suppressed in dHb precursors until it influences neuronal fate outcome during late stages of differentiation.

3.2 Premature induction of Wnt signaling perturbs Hb neurons differentiation

We found that Wnt signaling is likely kept in a silent state prior 36 hpf. Intuitively, we speculated that induction of Wnt signaling at these early stages could be rather harmful for habenular precursors. To explore this possibility, we prematurely activated Wnt signalling and observed the development of the habenular circuit. The *Et(-1.0otpa:mmGFP)*^{hd1} reporter line GFP labelles all Hb neurons and their projections toward the IPN as well as neighboring thalamic neurons in the pre-thalamus (Beretta et al., 2013; Beretta et al., 2017). Therefore this transgenic line enables a general overview of spatio-temporal key events in Hb circuit developent starting from 43 hpf time at which the GFP is firstly detected in the Hb (Beretta et al., 2017; Beretta et al., 2012; Beretta et al., 2013). In a series of experiments, *Et(-1.0otpa:mmGFP)*^{hd1} embryos were treated with the Gsk3β inhibitor LiCl for 30 min between 20 hpf and 32 hpf and subsequently fixed at 48 hpf (Fig. 7A, A',E and and Table S1). Intriguingly, embryos treated with LiCl between 24 and 26 hpf did not develop any GFP expressing habenular cells at 48 hpf (Fig. 7A-B', E and Table S1). Interestingly the loss of GFP neurons appeared specific for the Hb, as GFP positive neurons in the thalamus were largely unaffected as the overall morphology of the dorsal diencephalon as judged by nuclear staining (Fig. 7A, A'). In order to confirm that the observed effect was dependent on the manipulation of Wnt signaling, the same experiment was performed by using the Wnt activator BIO. Similarly, the continuous bathing of *Et(-1.0otpa:mmGFP)*^{hd1} embryos in the Wnt agonist between 22 and 28 hpf resulted in a critical reduction of GFP positive neurons in the habenulae at 48hpf as the one observed for LiCl (data not shown). Such a dramatic reduction of Hb neurons could be consequential to both a deficit in the establishment of the Hb precursor pool or the inability for dHb precursor to become differentiated neurons. To discriminate between these two possibilities, *Et(-1.0otpa:mmGFP)*^{hd1} embryos were treated with LiCl between 24 and 26 hpf and co-stained at 48hpf for the pan-neuronal

marker HuC/D and the endogenous GFP or alternatively stained for the habenular precursor marker *cxcr4b* (Roussigne et al., 2009). Intriguingly, while in treated

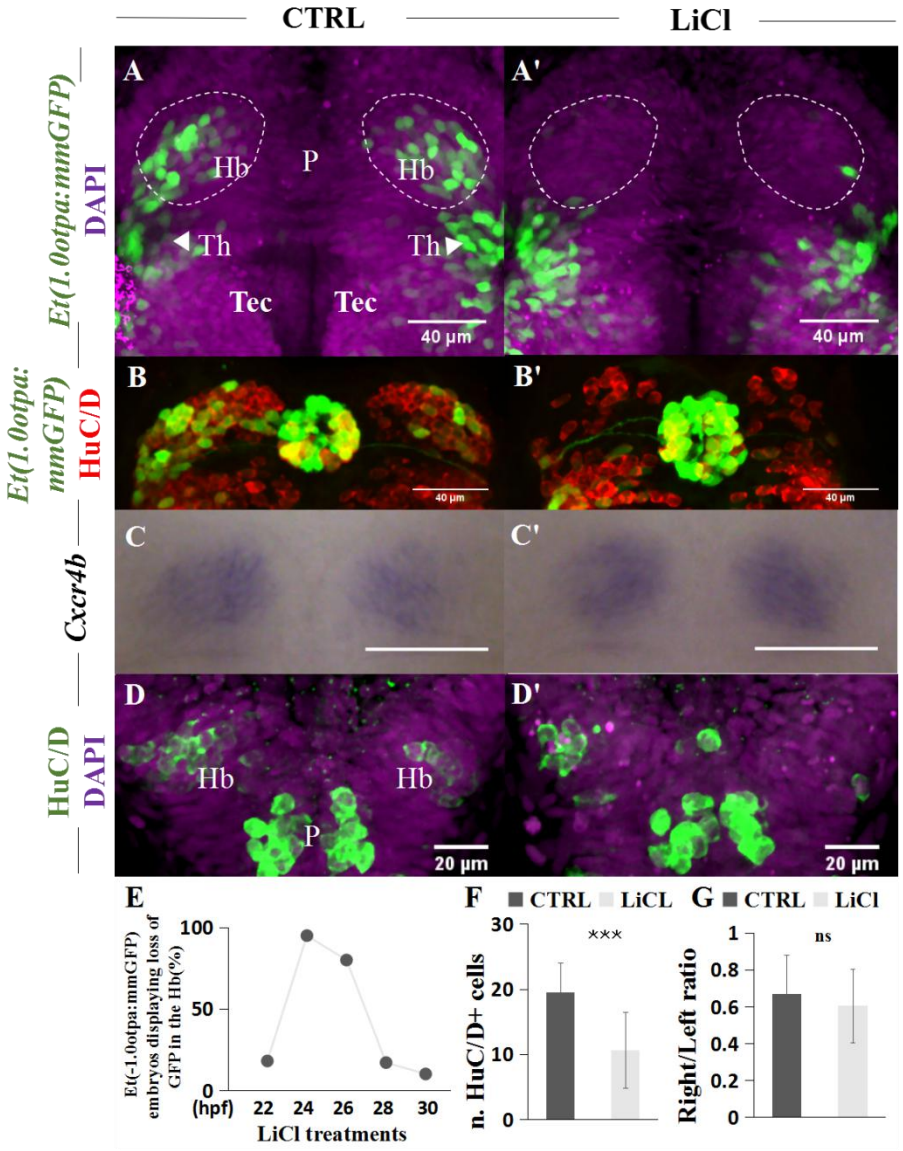

Figure 7: Premature activation of Wnt signaling delays habenular neuron differentiation.

(A-D') Dorsal views, anterior to the top focused onto the dorsal diencephalon of (A, B') Et(-1.0otpa:mmGFP) and (C, D') WT embryos at stages indicated. Nuclei are DAPI labeled. (A, B') Transient activation of Wnt signaling between 24 hpf and 26 hpf causes a loss of GFP expression at 48 hpf in habenular neurons of Et(-1.0otpa:mmGFP) transgenic embryos.(C,C',B, B', D,D',F,G) Expression of habenular precursor marker *cxcr4b* is largely unaffected while the number of HuC/D positive differentiating habenular neurons is strongly reduced at both 48 and 36 hpf, notably, their l-r asymmetric development remains unchanged. Hb, habenulae; P, pineal; ns, not significant; Tc, telencephalon; Tec, optic tectum; Th, thalamus.

embryos the reduction in GFP positive neurons was accompanied by a marked reduction in HuC/D positive cells (Fig. 7B, B' Table S2), the expression of the habenular precursor marker *cxcr4b* was largely unaffected (Fig. 7C,C' Table S2). Showing that the observed loss of GFP positive neurons is likely due to a reduction in the number of post mitotic habenular neurons. In order to confirm the above results and provide a precise quantification of the observed effect, we treated again embryos with LiCl and fixed them at 36hpf. At this stage, the number of HuC/D positive neurons is naturally lower so that stained neurons can be precisely counted. In line with the reduction observed at 48 hpf, the number of HuC/D positive neurons was significantly lower in treated embryos compared to controls (control: 19.5 +/-4.4, n=12; LiCl: 10,6 +/-5.8, n=12, p=0.0003)(Fig. 7D,D' and F). In contrast to this effect, the typical left bias in the onset of Hb neurogenesis was unaffected as also in LiCl treated embryos the number of HuC/D positive neurons was more abundant on the left side (control: 0.67 +/-0.53, n=12; LiCl: 0.6 +/-0.26, n=12, p=0.53)(Fig.2 D,D' and G). Also in this case the morphology of the diencephalon as well as the cell count of the adjacently developing pineal organ were indistinguishable from the control group (control: 20.71 +/-1.60, n=7; LiCl: 21.13 +/-1.73, n=8, p=0.64). Taken together these observation suggest that Hb precursors need to be protected from the activation of Wnt signaling prior to 36 hpf, as premature activation of the pathway result in Hb precursor to fail entering their differentiation program.

3.3. Delayed neurogenesis affects asymmetric dHb neuron differentiation

Transient induction of Wnt signalling between 24 and 26 hpf results in a marked reduction of differentiated Hb neurons at 48 hpf. In order to investigate the destiny of these few differentiating neurons we monitored habenular development at a later developmental stage by using the *Et(-1.0otpa:mmGFP)*^{hd1} reporter. Interestingly, at 72hpf, LiCl treated embryos displayed GFP expression in the habenulae even if slightly reduced (Fig. 8A, A'). This suggests that first, neurons still acquire the dHb

fate and that second, the reduction observed at 48hpf is likely caused by a marked delay in the timing of neurogenesis. Habenular neurons are typically generated via

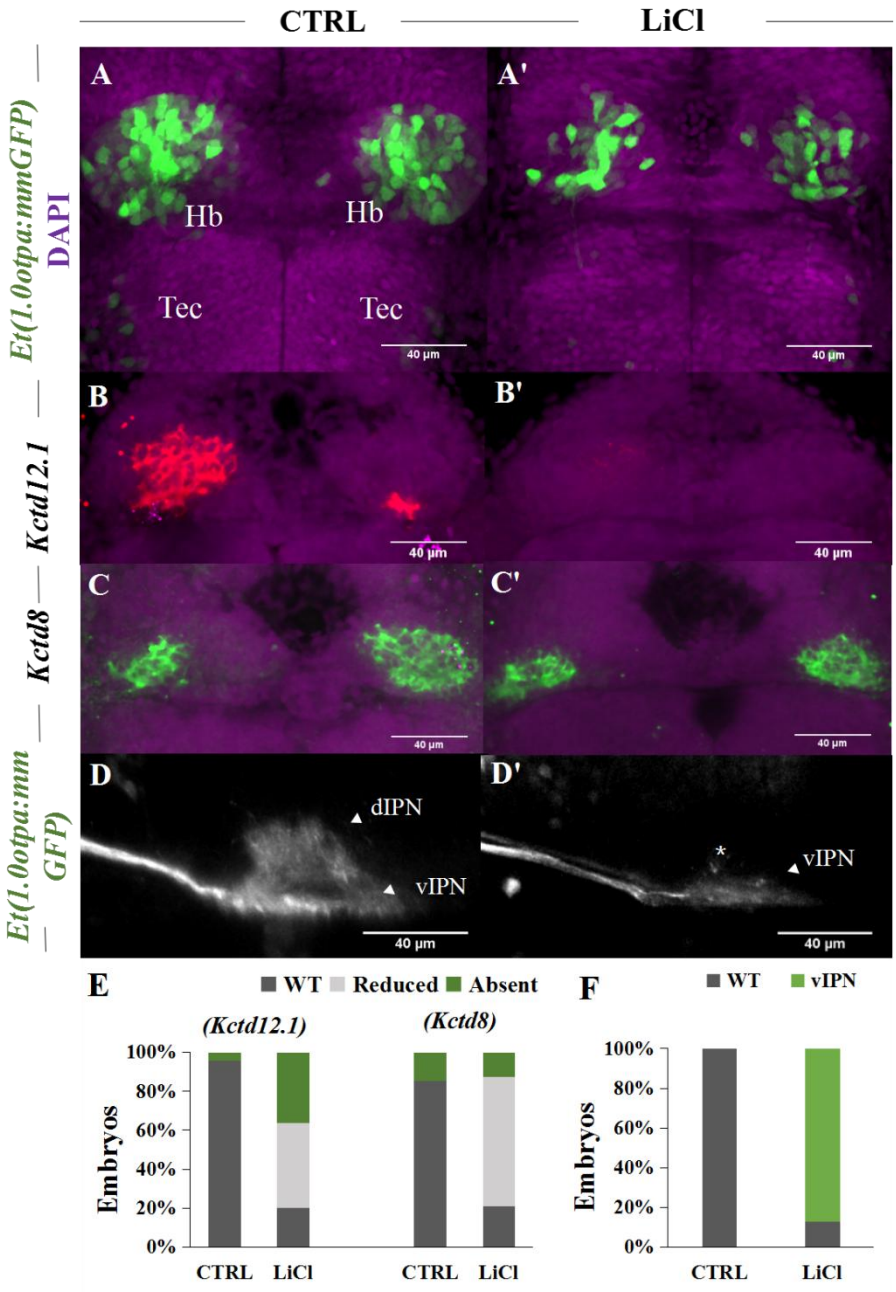

Figure 8: Premature Wnt signaling causes a reduction of dHbl neurons and symmetric IPN innervation

(A-C') Dorsal views, anterior to the top focused onto the dorsal diencephalon of (A, A', D, D') Et(-1.0otpa:mmGFP) and (B-C') wild type embryos at 3 dpf. Nuclei are DAPI labeled. (A, A') LiCl treated Et(-1.0otpa:mmGFP) embryos show delayed habenular neuron differentiation. (B-C', E) Accordingly, markers for both the (B, B') dHbl and (C, C') less severely also dHbm neurons are reduced. (D, D', F) Lateral views of IPN innervation by habenular efferent axons, anterior to the left. Treated embryos show a consistent innervation of only the vIPN indicating the generation of predominantly dHbm neurons. d, dorsal; Hb, habenula, IPN, interpeduncular nucleus; Tec, optic tectum; v, ventral.

two subsequent differentiation waves (Aizawa et al.,2007). The different timing at which Hb neurons are born is closely related to their subsequent destiny, so that neurons born during the second wave have an higher likelihood to become dHbm neurons. Therefore we expected that premature activation of Wnt signaling would consequently result in Hb precursors to acquire the dHbm rather than the dHbl. To explore this possibility, we stained treated embryos with the dHbl maker *kcdt2.1* and the dHbm marker *kcdt8* at 72hpf. Interestingly, while the expression of *kcdt2.1* was nearly abolished, the dHbm marker *kcdt8* was only mildly reduced (Fig. 8B-C', E and Table S2.). The same trend was followed by the dHbl marker *Et(gata2a:EGFP)*^{pku588} (Fig. 8A,A' and Table S2) and the dHbm marker *Tg(hsp70-brn3a:GFP)*^{rw0110b} (Fig. 8B,B' and Table S2). Further suggesting that as a consequence of their delayed differentiation, most dHb precursors might acquire characteristics typical of dHbm neurons at the expenses of dHbl neurons. In order to unambiguously confirm these observations we looked at habenular projection in the *Et(-1.0otpa:mmGFP)*^{hd1} as dHbm neurons are typically innervating the vIPN, while dHbl neurons innervate the dIPN. Intruguingly, in treated *Et(-1.0otpa:mmGFP)*^{hd1} embryos both left and right dHb axons were innervating the vIPN instead of segregating along the dorso-ventral axis confirming their dHbm origin (Fig. 8D,D', F and Table S3). However, it is still possible that early induction of Wnt signalling could directly affect IPN development and thereby influence the distribution of afferent axons. The IPN can be typically identified by the expression of *somatostatin 1* (*sst1*), which has been used as an indicator of structural IPN integrity (Beretta et al., 2017). In order to sort out whether in treated embryos the IPN was developing normally or not , *Et(-1.0otpa:mmGFP)*^{hd1} embryo were simultaneously stained for s*st1* and the endogenous GFP. Interestingly, symmetric vIPN innervation was correlating with an overall normal expression of *sst1*(Fig. 9C,C' and D,D'). We only noted that in LiCl treated embryos the expression of *sst1* was partially extended posteriorwards likely due to a slight developmental delay (Fig. 9D,D'). We also excluded that our results may have originate from a defect in parapineal cell migration, as parapineal ablation prior 30hpf has been proven to result in the development of a double right habenulae (Concha et al., 2003, Gamse et al., 2003, Gamse et al., 2005). However in LiCl treated embryos the leftward migration of the parapineal was never affected (data not shown). We concluded that early suppression of Wnt signaling is required for Hb precursors to undergo early differentiation into dHbl neurons. Indeed premature Wnt pathway activation causes

dHb precursor cells to skip the first differentiation wave and differentiate into dHbm neurons (Fig. 9E).

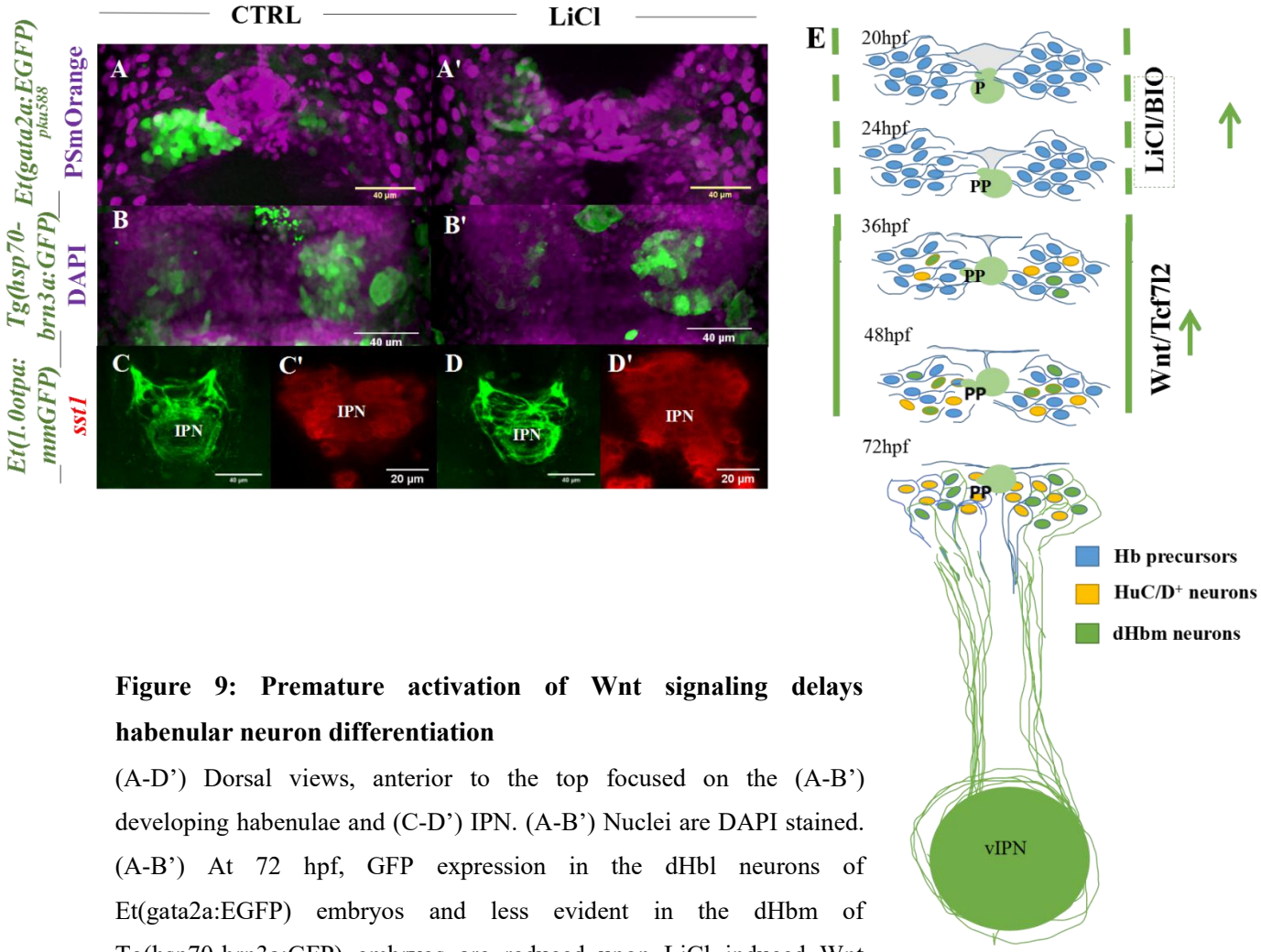

Figure 9: Premature activation of Wnt signaling delays habenular neuron differentiation

(A-D') Dorsal views, anterior to the top focused on the (A-B') developing habenulae and (C-D') IPN. (A-B') Nuclei are DAPI stained. (A-B') At 72 hpf, GFP expression in the dHbl neurons of Et(gata2a:EGFP) embryos and less evident in the dHbm of Tg(hsp70-brn3a:GFP) embryos are reduced upon LiCl induced Wnt signalling activation. (E-F') Habenular efferent axons innervate the ventral IPN only in the presence of largely normal expression of somatostatin1 in the IPN of Et(-1.0otpa:mmGFP) embryos.(E) Summary of events during Hb circuit development: LiCl and BIO treatments cause a delay in Hb precursor (blu) differentiation into HuC/D post mitotic neurons (yellow). As a consequence neurogenesis is delayed, Hb neurons acquire the dHbm character and they bilaterally innervate the vIPN. PP, parapineal; IPN, interpenduncular nucleus; Hb, habenulae; d, dorsal.

3.4 *Wif1* is expressed in the presumptive habenulae during Hb neuron differentation

Our result suggest that Wnt/beta-catenin pathway components required for signaling activity are expressed in early habenular precursors. These components must be kept inactive to allow the precursors to differentiate early into dHbl. Therefore it is conceivable that habenular precursors need a mechanism to protect themselves at early stages from incoming Wnt ligands. The wnt inhibitor factor 1 (Wif1) is a secreted molecule that binds to Wnt ligands and inhibits their interaction with the

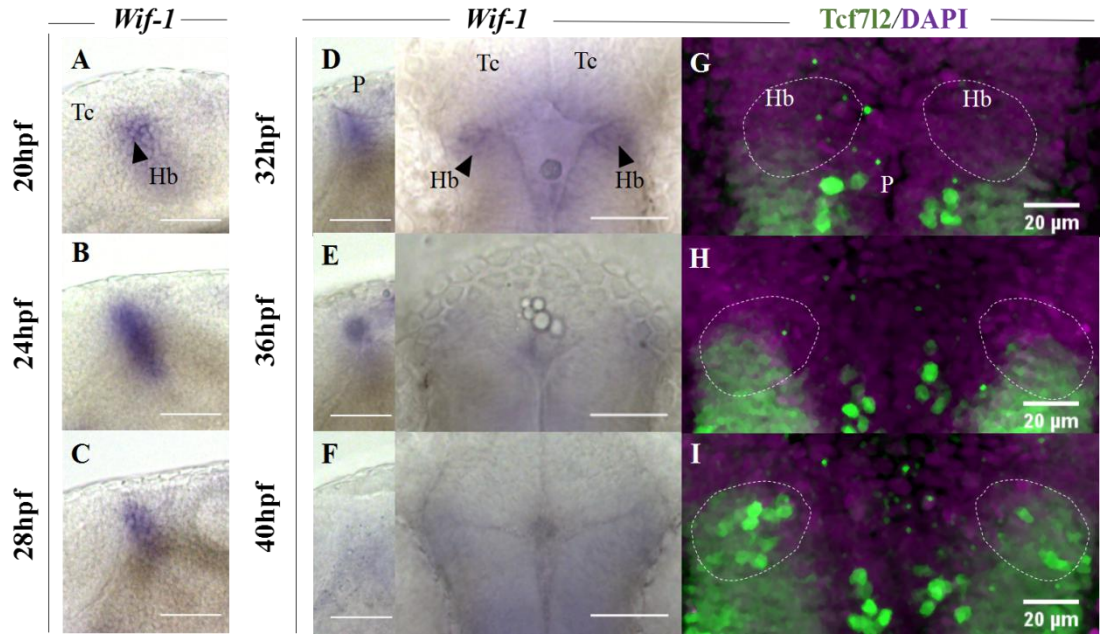

Figure 10: *Wif1* expression temporally complements Tcf7l2 expression and habenular neuron generation

(A-C) and (D-F left) lateral views, anterior to the left and (D-F right) and (G-I) dorsal views with anterior to the top focused on the diencephalon of wild type embryos at stages indicated. *Wif1* is discretely expressed in the developing habenular region (arrowheads) until Tcf7l2 expression is initiated at 36 hpf and influences dHb neuron differentiation (Hüsken et al., 2014). Hb, habenula; P, pineal; Tc, telencephalon.

frizzled/LRP receptor complex. Wif1 can directly bind to canonical and non-canonical Wnt ligands (Wnt3a, Wnt4, Wnt5a, Wnt7a, Wnt8, Wnt9a, Wnt11) (Hsieh et al., 1999; Kawano and Kypta, 2003) and does so in different developmental and pathological contexts. Indeed, Wif1 function has been linked to mainly lung, bone and tooth formation besides being a crucial oncogene linked to the formation of various tumors (Kansara et al., 2009; Lee et al., 2015; Ramachandran et al., 2012; Wissmann et al., 2003; Xu et al., 2011). Importantly, we found that *wif1* is bilaterally expressed in the presumptive habenulae during the time at which Hb neurons differentiate and displays a striking spatio-temporal pattern (Fig. 10A-F). Indeed, *wif1* is expression starts around 20 hpf, increases at around 24 hpf and subsequently progressively shades away and is undetectable between 36-38 hpf (Fig. 10A-F). Interestingly, this is exactly the time in which the levels of Wnt signaling are rising up to impose the dHbm character on post mitotic dHb neurons (Hüsken et al., 2014). As the transcription factor Tcf7l2 is the principal mediator of this late role of Wnt signalling, we compared the expression pattern of Tcf7l2 with the one of *wif1*. In line with previous observations we found the expression of these genes largely complementary, indeed the disappearance of *wif1* expression is paralleled by a progressive increase in Tcf7l2 expression in the habenulae (Fig. 10G-I). This strongly suggest that *wif1* may be the likely antagonzer of Wnt signaling during the early stages of habenular neuron development.

3.5 Wif1 knockdown phenocopies early Wnt activation

wif1 is expressed in the developing habenulae at the time at which Hb precursors need to be protected from upcoming Wnt ligands. Therefore it is possible that *wif1* may be the likely inhibitor involved in this process. If this is the case, loss of w*if1* may result in a very similar phenotype to the one observed upon LiCl and BIO treatments. Notably, w*if1* is expressed starting already at gastrulation stages in the paraxial mesoderm and plays a pivotal role in posterior axis formation (Hsieh et al., 1999; Thisse and Thisse, 2005). Therefore, to avoid early embryonic malformations, we chose to analyze embryos hypomorphic for *wif1* using an established *wif1* morpholino

(Yin et al., 2012). Also in this case we use the *Et(-1.0otpa:mmGFP)*^{hd1} transgenic line as it proved to be a very powerful read-out for Hb circuit development. Intriguingly, morpholino injection into these embryos resulted in a loss of GFP positive neurons in the habenulae at 48hpf very similar to what we had observed with drug treatments (Fig. 11A-B' and Table S4). Also in this case, the effect appeared to be very specific as the expression of GFP in neighboring thalamic neurons was unaffected as well as the overall morphology of the habenular nuclei, as shown by the DAPI staining (Fig. 11A-A'). We therefore investigated whether the observed reduction was also in this case caused by a reduction of differentiated neurons. Interestingly, at 48 hpf, HuC/D expressing differentiating habenular neurons were strongly reduced in *wif1* morphants

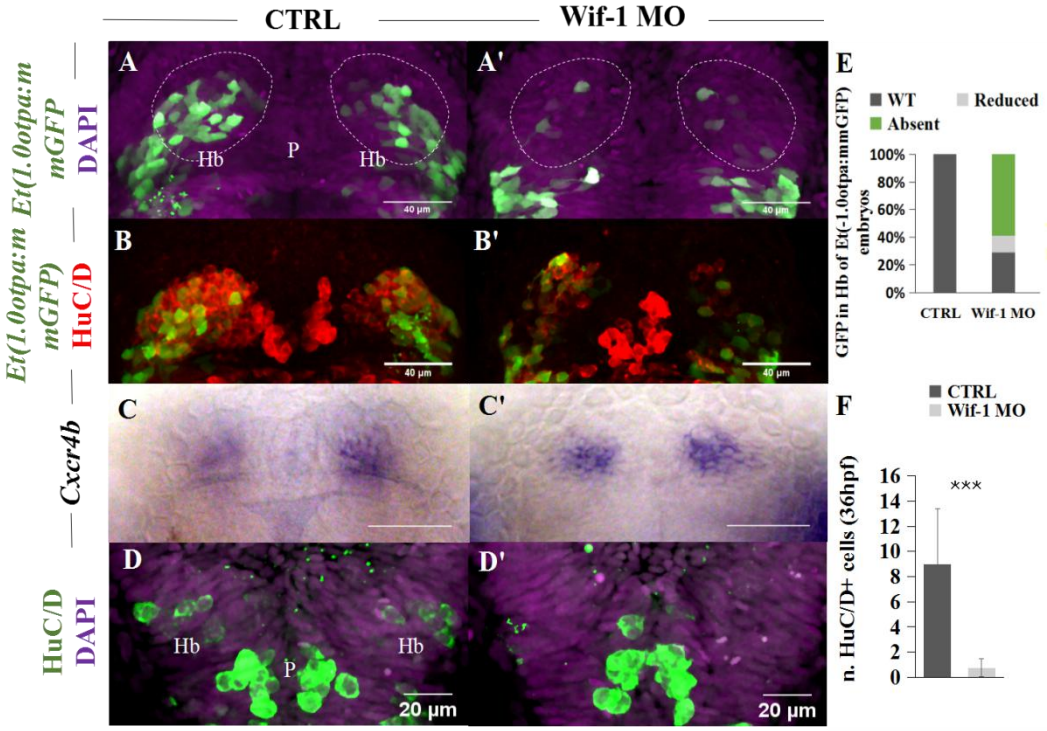

Figure 11: Wif1 knock down mimics the effects of premature transient activation of Wnt signaling

(A-D') Dorsal views, anterior to the top focused onto the dorsal diencephalon of (A, B') Et(-1.0otpa:mmGFP) and (C, D') wild type embryos. Nuclei are DAPI labeled. (A-C') At 48 hpf, *Wif1* morphant embryos exhibit the lack of GFP in the habenulae in Et(-1.0otpa:mmGFP) transgenic embryos and a reduction in HuC/D positive differentiating neurons in the presence of largely unaffected *cxcr4b* expression in habenular precursor cells (Roussigne et al., 2009). (D,D', F) Wif1 hypomorphic embryos exhibit strong reduction of HuC/D positive neurons at 36hpf.Hb, habenulae; P, Pineal.

(Fig. 11B-B' and Table S4). Conversely, the expression of the precursor marker *cxcr4b* was unaffected (Fig. 11C-C' and Table S4) as well as the leftward migration

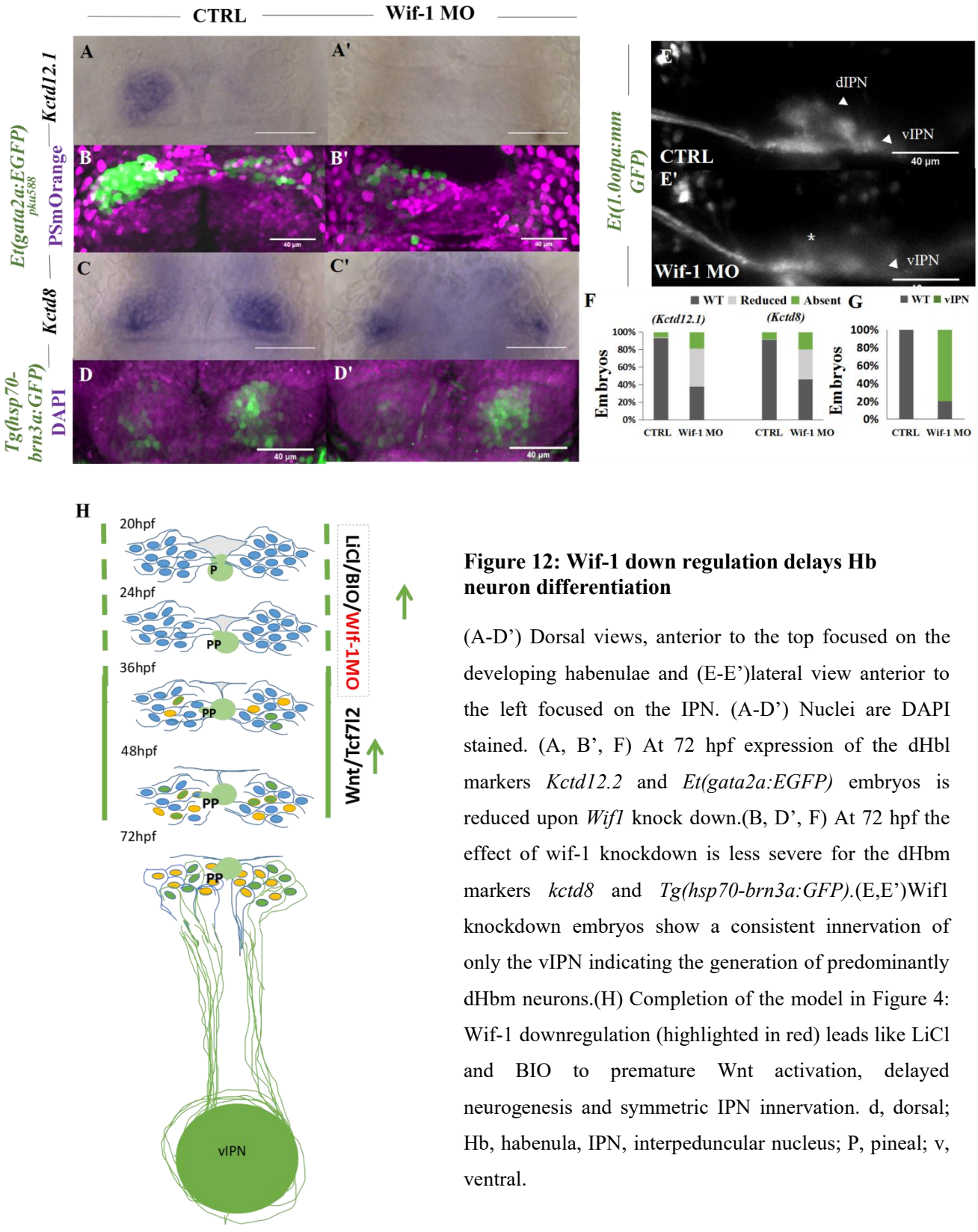

Figure 12: Wif-1 down regulation delays Hb neuron differentiation

(A-D') Dorsal views, anterior to the top focused on the developing habenulae and (E-E')lateral view anterior to the left focused on the IPN. (A-D') Nuclei are DAPI stained. (A, B', F) At 72 hpf expression of the dHbl markers *Kctd12.2* and *Et(gata2a:EGFP)* embryos is reduced upon *Wif1* knock down.(B, D', F) At 72 hpf the effect of wif-1 knockdown is less severe for the dHbm markers *kctd8* and *Tg(hsp70-brn3a:GFP)*.(E,E')Wif1 knockdown embryos show a consistent innervation of only the vIPN indicating the generation of predominantly dHbm neurons.(H) Completion of the model in Figure 4: Wif-1 downregulation (highlighted in red) leads like LiCl and BIO to premature Wnt activation, delayed neurogenesis and symmetric IPN innervation. d, dorsal; Hb, habenula, IPN, interpeduncular nucleus; P, pineal; v, ventral.

of the parapineal (data not shown). We then proceeded with the quantification of the observed effect, Wif1 morphants were fixed at 36 hpf and HuC/D positive neurons were counted. As observed in LiCl treated embryos, *wif1* down-regulation resulted in a very significant reduction in the number of HuC/D positive cells (control: 9.14 +/-4.6, n=7; Wif1 Mo: 0.38 +/-0.74, n=9, p<0.0001) (Fig. 11D-D') whereas both the morphology of the dyencephalon and the number of the neighboring pineal cells appeared unaffected (control: 12.63 +/-1.51, n=8; Wif1Mo: 11.88 +/-1.46, n=11, p=0.328)(Fig. 11D-D'). These results s uggest that indeed *wif1* down-regulation likely result in increased levels of Wnt signalling within the habenular precursor anlage. To further prove this point we asked whether the reduction of wif1 influences the destiny of Hb neurons towards the dHbm character and stained Wif1 morphants for the different dHbl and dHbm markers at 72hpf. Overall, the expression of the dHbl markers *Kctd12.1* and *Et(gata2a:EGFP)*^{pku588} was strongly reduced (Fig. 12A-B', F and Table S4) compared to the dHbm markers *Kctd8, Kctd12.2* and *Tg(hsp70-brn3a:GFP)*(Fig. 12C-D',F and Table S4). However some of the dHbm markers, as for instance *Kctd8,* was not as reduced as upon LiCl treatments (Table S2-S4). Considering this we analysed the innervation pattern of dHb axons in wif1 hypomorphic condition. Notably, dHb axons were targeting exclusively the vIPN in *Et(-1.0otpa:mmGFP)*^{hd1} wif1 hypomorphic embryos (Fig. 12E,E' and TableS3). These data suggest that Wif1 is the central mediator of early suppression of Wnt/beta-catenin in habenular precursor cells. Lack of Wif1 results in premature activation of the pathway, a delay in habenular neuron specification and their subsequent development into dHbm neurons on both sides of the brain (Fig. 12H).

3.6 Wnt/beta-catenin signaling functions in a feedback loop to shield dHb precursors

Wif1 is expressed in close proximity to the MDO, which is a source of Wnt signaling patterning the pre-thalamus and thalamus (Hagemann and Scholpp, 2012; Cavodeassi and Houart, 2012). Ligands emanating from the organizer are likely inducing specific transcriptional programs also in the dorsally positioned habneular precursors cells. We speculated that the expression of *wif1* could be induced or modulated by Wnt signaling. In support of this hypothesis, previous studies showed that Wnt signaling can negatively or positively regulate itself during certain processes in development and disease (Licchesi et al., 2010; Cowling et al., 2007). The self-regulation often involves a variety of molecules, which can include Wif1 (Zirn et al., 2006; Diep et al., 2004; Vaes et al., 2005; Boerboom et al., 2006). To clarify this point, we used different approaches to modulate Wnt signaling levels during development and assessed whether the expression of *wif1* was consequently affected. In the *tg(hsDkk1:GFP)* transgenic line, ectopic over-expression of the Wnt inhibitor Dkk1 can be triggered at defined time points by providing a prolonged 37C° heat shock (Stoick-Cooper et al., 2007). Dkk1 was induced starting from 22hpf and the resulting GFP positive embryos as well as the GFP negative non-transgenic control embryos were fixed at 25 hpf. Intriguingly, in the large majority of the GFP positive embryos, *wif1* expression appeared strongly reduced (Fig. 13B; Table S5) compared to controls (Fig. 13A). In order to further confirm this result and assess the Wnt dependence of the observed effect, Wnt down-regulation was induced further downstream in the pathway by using the Wnt inhibiting drug IWR. This drug is stabilizing Axin1 and therefore promoting β-catenin degradation. We find that also IWR-mediated inhibition of Wnt signalling at 22hpf for 3hr resulted in reduced *wif1* expression at 25hpf (Fig. 13C and Table S5). Tcf7l2 binds to β-catenin to induce Wnt downstream genes downstream Axin-1 (Carl et al., 2007, Hüsken et al., 2014). Interestingly, in Tcf7l2 mutants *wif1* expression appeared not to be affected (Fig. 13D). The likely explanation is that at these early stages Tcf7l2 is not expressed in the habenulae and therefore *wif1* expression may be induced under the control of another member of the Tcf transcription factor family. These results show that *wif1* expression is modulated by Wnt signalling and prompted us to explore the reverse approach and assess

putative changes in *wif1* expression upon Wnt up-regulation. To obtain transient up-regulation of the pathway, embryos were treated with LiCl for 30 min at 22 hpf and fixed at 25 hpf in analogy to the Wnt downregulation experiments. Strikingly, we found the expression of *wif1* to be markedly increased (Fig. 13F and Table S5). The very same effect was observed when embryos were bathed in the Wnt activating drug BIO, also starting from 22hpf (Fig. 13E and Table S5). To observe whether this phenomenon was reproduced in a mutant background we assessed the expression of *wif1* in *axin1*$^{-/-}$ embryos in which a mutation in the GSK3beta binding site in Axin-1 leads to constitutive activation of the Wnt signaling pathway. Also in this case the

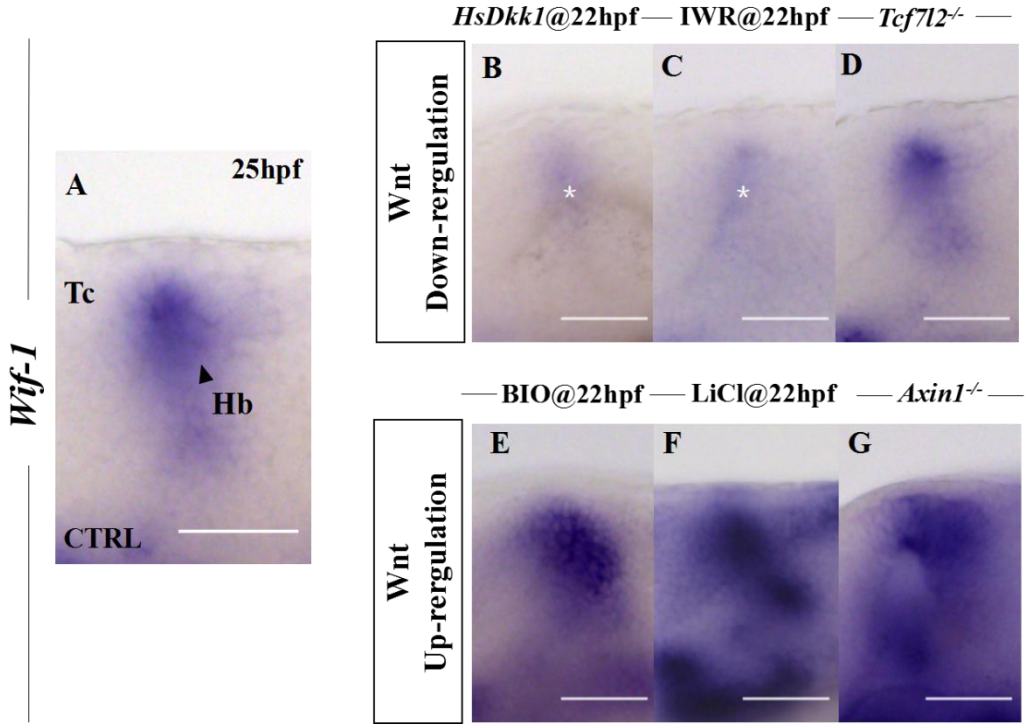

Figure 13: *Wif1* expression is regulated by Wnt signaling

(A-G) Lateral views with anterior to the left focused on the diencephalon at 26 hpf labeled for *Wif1* expression. (A-D) Wnt downregulation results in a decrease of *Wif1* expression in the habenulae (asterisks in B, C) with the exception of *Tcf7l2* mutant embryos, which is consistent with the temporally complementing expression of Tcf7l2 and *Wif1*. (E-G) Wnt upregulation causes an increase in Wif1 expression. Hb, habenula; Tc, telencephalon.

expression of *wif1* was increased at 25hpf further proving a positive regulation of *wif1* by Wnt signalling (Fig. 13G and Table S5). Notably, *Wif1* expression is persistent till 36 hpf. Therefore it is possible that positive regulation by Wnt signalling may be active throughout the whole period of *wif1* expression. In order to evaluate if this is the case, Wnt down- and up-regulation was induced 10 hours later by using the different approaches reported above but embryos were fixed at 34 hpf. Notably, also in this case the expression of *wif1* was induced by the increase in Wnt signalling (data not shown). These findings demonstrate that Wif1 is part of a Wnt regulatory feedback loop, which may buffer habenular precursor cells from extracellular Wnt ligands.

3.7 Ectopic overexpression of the Wnt8 ligands does not markedly affect dHb neuron differentiation

Wnt inhibition via IWR mediated stabilization of Axin-1 or via ectopic overexpression of Dkk1 results in a marked reduction of *wif1* expression. Conversely, up regulation of Wnt signalling via inhibition of Gsk3β or in Axin-1 mutants results in the increase in *wif1* expression. Therefore we speculated that early suppression of Wnt signaling is occurring via a Wif1 mediated feedback inhibition. If our hypothesis is correct premature activation of Wnt signalling should be buffered by an increase in *wif1* expression enabling Hb precursor to proceed toward their differentiation program. However upon BIO and LiCl treatments the resulting increase in *wif1* expression is not capable to rescue the observed delay in Hb neuron differentiation. One possible explanation is that both LiCl and BIO are inhibiting Gsk3β which is acting downstream the ligand/receptor complex. In this scenario, the activation state of the Wnt signaling pathway would become insensitive to any secreted factor, either ligand or inhibitor like *wif1*. To confirm this hypothesis we up-regulated Wnt signalling at ligand level by using the *tg(hsp70l:Wnt8a-GFP)* transgenic line which enables activation of Wnt signalling up-stream the receptor complex (Weidinger et al., 2005).

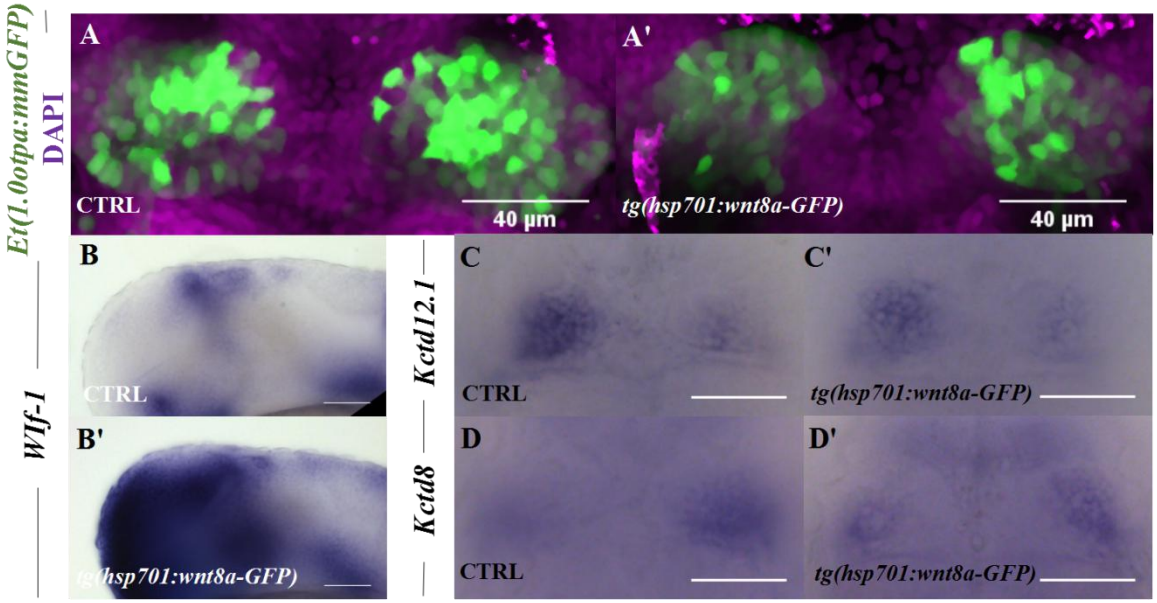

Figure 14: Transient extrinsic activation of Wnt signaling has no major effect on dHb development

(A, A', C-D') Dorsal views with anterior to the top focused on the diencephalon at stages indicated. (B, B') Lateral view, anterior to the left focused on the head region. Heat shock activation of *Wnt8* expression strongly induces *Wif1* expression but has no major effect on (A, A') Et(-1.0otpa:mmGFP), (B, B') *Kctd12.1* or (C, C') *Kctd8* expression in habenular neurons.

Initially we assessed whether ectopic overexpression of the wnt8 ligand would trigger an increase of *wif1* expression at 25 hpf. Surprisingly, heat-shock induction resulted in a dramatic enlargement of the *wif1* expression domain, spanning throughout the entire embryo including the habenulae (Fig 14B,B' and Table S5),. However, in line with our hypothesis, these embryos exhibited no gross abnormalities in both GFP expressing dHb cells and IPN innervation pattern as shown by the *Et(-1.0otpa:mmGFP)*^{hd1} reporter line (Fig. 14A,A'). Also, the overall expression of *kctd12.1* and *kctd8* appeared very similar to the control (Fig. 14C-D' and Table S6). These findings are consistent with the idea that unlike the intracellular activation of the pathway, extracellular Wnt ligands can be compensated for by increased Wif1 levels. It still remains to elucidate what mechanism underlies the temporal control of

decreasing Wif1 expression, which allows subsequently to influence dHb neuronal fate

3.8 Wif1 is transiently expressed in the presumptive IPN

Wnt signalling needs to be suppressed in habenular precursors to allow their temporally defined differentiation into the different neuronal subtypes. This suppression is achieved trough Wif1, which acts like a guardian to shield precursors from Wnt ligands and does so via feedback inhibition of the Wnt pathway. Interestingly, we found that *wif1* is also expressed in the presumptive IPN from around 40 hpf (Fig. 15A,A'). By looking at *wif1* expression time course, we noted that while the expression of the gene is initially very strong, its levels are progressively shading over time so that at 72hpf its expression is nearly undetectable (Fig. 15B). Also Wnt ligands are expressed around this time in the IPN like for instance *wnt8b* which is found in the presumptive IPN region around 48hpf (Thisse and Thisse, 2005; Thisse and Thisse, 2008). Importantly, the timing of *wif1* and Wnt ligand expression in the IPN corresponds to the timing of IPN innervation by dHb efferent axons. Hence we speculated that perhaps, as in the dHb, suppression of Wnt signaling would be required for IPN precursors to enter their neuronal lineage. The maturation state of IPN cells, in turn might have an influence on the approaching Hb efferent projections. In order to explore this exciting hypothesis we performed a series of preliminary experiments in which we used LiCl to activate Wnt signaling at 48 hpf in *Et(-1.0otpa:mmGFP)*^{hd1} transgenic embryos. We choose this time-point as Wnt activation is unlikely to affect neurogenesis in the habenulae at these late stages. Interestingly, in the 40% of the treated embryos the innervation of the IPN was critically impaired or absent (n=20) at 72hpf (Fig. 15C-D). These preliminary data suggest that Wif1 may control the level of Wnt signalling not only in the Hb but also in the IPN and in this way tuning the overall wiring of the habenular circuit. However further experiments will be required for getting further insight into this fascinating mechanism.

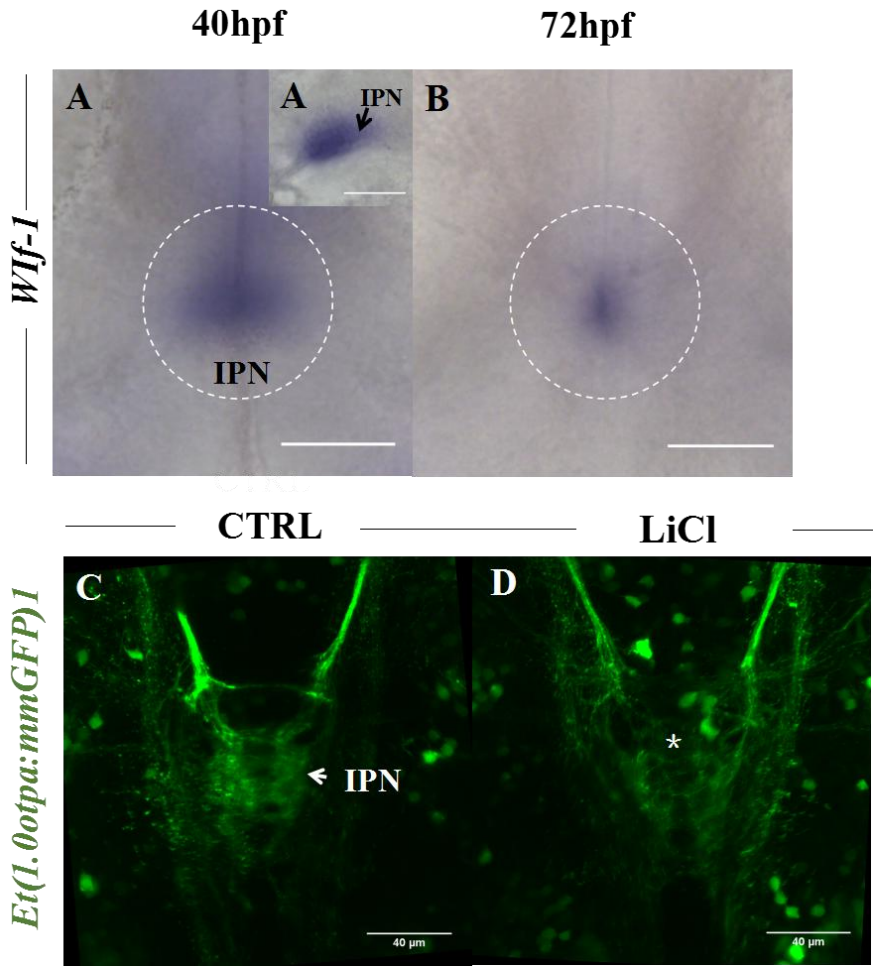

Figure 15: Possible involvement of the Wnt signaling pathway in the development of the IPN

(A, A', C-D) Dorsal views with anterior to the top focused on the IPN at stages indicated. (A,B) *Wif-1* is expressed in the presumtive IPN and its expression progressively decreases over time. (C,D) Wnt signalling activation at 48hpf via LiCl on *Et(-1.0otpa:mmGFP)* embryos result in loss of IPN innervation at 72hpf. IPN, interpenduncular nucleus.

3.9 Generation of the *wif1* mutant via Crispr/cas9 mediated genome editing

The knockdown of the *wif1* gen*e* obtained via an established morpholino allowed us to uncover its Wnt modulating function within the developing epithalamus. In order to implement and further confirm our morpholino based data-set we used the CRISPR/Cas9 technology to generate a *wif1* Knock out (Hwang et al., 2013; Auer et al., 2014; Hisano et al., 2015) The wif1 protein is composed of a WIF (Wnt inhibitory factor) superfamily domain at the N-terminal and five EGF repeats at the C-terminal (Hsieh et al., 1999). For our CRISPR approach we decided to target the WIF domain, on one hand to specifically inhibit the ability of wif1 to bind to Wnt ligands and on the other to avoid the possible onset of compensatory mechanisms. In order to predict the best gRNAs targeting within the first 4 exons of the *wif1* gene (which encode for the WIF domain) we used the CCTop target predictor (Stemmer et al., 2015) and we selected two different gRNAs targeting the second exon *gWifE2* and the forth exon *gWifE4 (*see section 5.11.1 in experimental procedures for target sequences). In order to test the efficiency of both gRNAs, *gWifE2* or *gWifE4* were injected together with the Cas9 mRNA in the cytoplasm of 1 cell stage WT zebrafish embryos. Cas9 mediated DSBs (double strand breaks) result in a mosaical range of different genomic modification within the same FO embryo, which makes the analysis of gRNA efficiency rather complicated. In order to overcome this problem we analyzed our freshly injected embryos using the Illumina MiSeq technology (Gagnon et al., 2014) (in colaboration with Dr. Ana Faro in Steve Wilson lab, UCL, London, UK). Indeed, by enabling single molecule sequencing, the MiSeq provide an overview of the entire range of Cas9 mediated modifications that occurred within a specific locus (Gagnon et al., 2014). Briefly, genomic DNA was extracted from pools of 10 injected embryos vs controls and the *gWifE2* or *gWifE4* target sequences amplified by using MiSeq primer tags. Amplicons were finally sequenced with the MiSeq sequencer. Intriguingly, data analysis revealed that the *gWifE2* was able to specifically induce DSBs at the predicted cutting site. Notably within the 1050 output reads, 32% displayed SNPs and deletions of different lengths (From 1bp to 44bp), while in the control group all the reads were unaffected (Fig. 16A). Similarly, for the *gWifE4* we found that on a total of 2639 reads 39% were also displaying SNPs and deletions of

different lengths (from 2 to 54 bp) while the control group was free from any modification (Fig. 16B). We concluded that both gRNAs were inducing DSBs with a

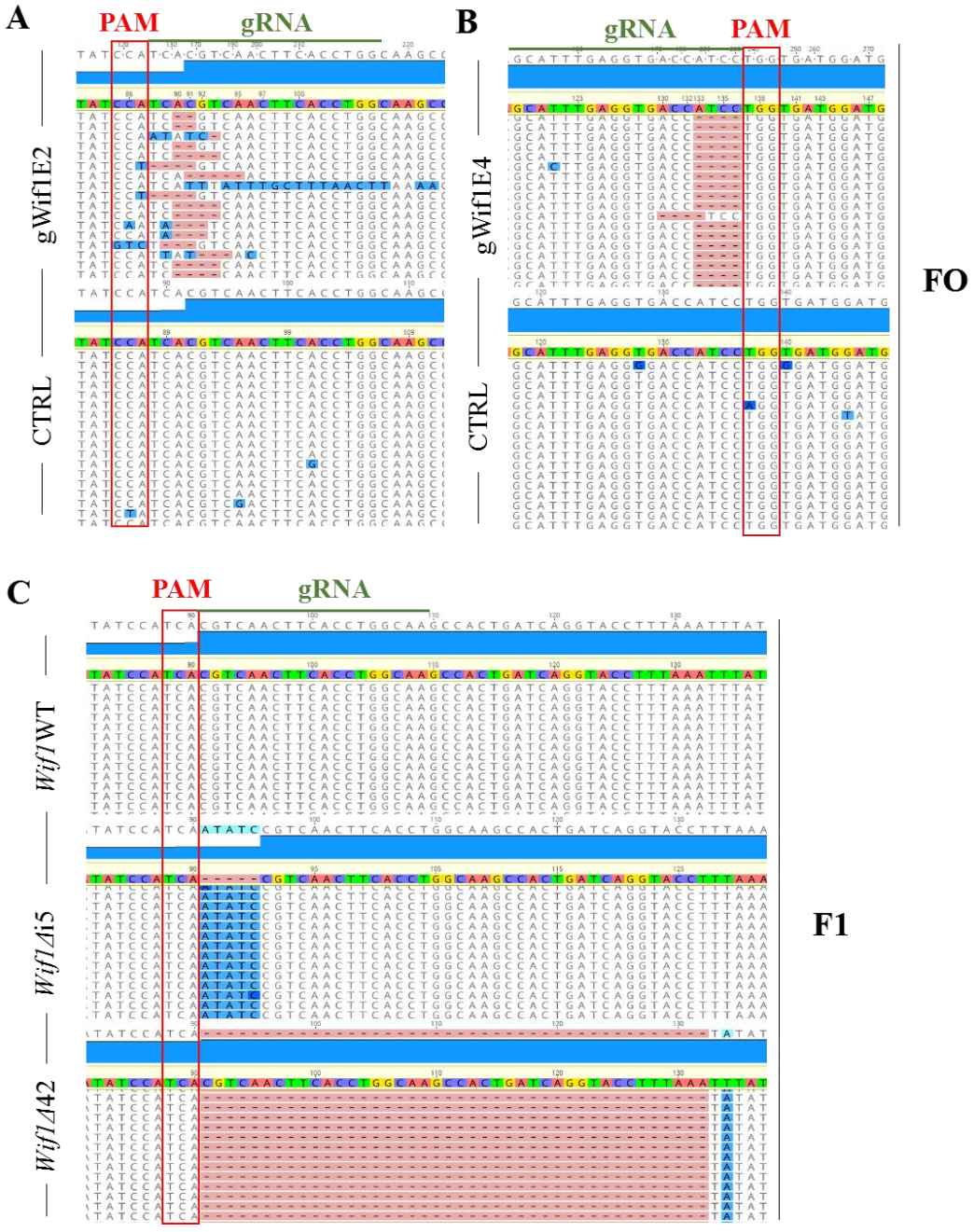

Figure 16: Crispr/Cas9 mediated generation of *wIf1* mutant alleles

(A,B) FO embryos injected with the gWif1E2 and gWif1E4 display genomic alterations at the predicted cutting site.

(C)gWifE2 induced allelic variants are inherited by the F1 generation

good efficiency. For the establishment of the mutant line we decided to use the *gWifE2* as it is targeting the WIF domain at its core. Therefore we performed again *gWifE2* injections, but this time into embryos of the reporter line for the habenulae *Et(gata2a:EGFP)*^{pku588} and allowed them to develop under standard conditions. In order to identify putative carriers, F0 adults we crossed with WT fish and from each cross 10 single embryos were screened for the presence of inherited mutant alleles. For the screening we used again the MiSeq approach, as it proved to be particularly sensitive. Intriguingly we identified two FO carriers transmitting a different allele to the F1 generation. In one case a mutant allele carrying a 5bp insertion (*Wif1Δi5*) downstream the PAM sequence and in the other an allele with a 42bp deletion (*Wif1Δ42*) also downstream the PAM (Fig.16C). These results suggest that CRISPR approach was successfully enabling germ line transmission of *Wif1* mutant variants, yet validation of these data via restriction analysis is still required and will be readily performed as well as the characterization of the two different alleles.

4. Discussion

4.1 Early events in habenular neurogenesis require tight modulation of Wnt signalling

The first evidences linking Wnt signaling to fate specification of dHb neurons comes from the analysis of *axin-1* mutants (Heisenberg et al., 2001, Carl et al., 2007). Axin-1 is classically functioning within the β-catenin destruction complex where it ensures β-catenin degradation in the absence of Wnt ligands. (Caneparo et al., 2007; De Stropera and Annaert, 2001). In these mutants, Axin-1 carries a mutation in the GSK3β binding domain leading to constitutive activation of the pathway and likely persistent β-catenin mediated gene induction (Heisenberg et al., 2001). In the mutant background the habenulae develop with a symmetric double right character, in which mainly dHbm neurons are generated and exclusively innervate the ventral IPN (Carl et al., 2007). In support of these first evidences, a forward genetic screen led to the identification of Tcf7l2, a transcriptional regulator of Wnt signaling, as a key modulator of habenular asymmetries (Hüsken et al., 2014). Interestingly, contrary to what is observed in *Axin-1* mutants, in *tcf7l2* mutants the habenulae develop with a double left character in which neurons are bilaterally innervating the dIPN (Hüsken et al., 2014). Therefore, Tcf7l2 was proven to be the fundamental mediator of dHb neuron differentiation into dHbm and its action defined within a critical time window between 34 and 36 hpf (Hüsken et al., 2014). So far these results were confining the involvement of Wnt signaling in the fate specification of post-mitotic dHb neurons. Intriguingly we now provide evidences that Wnt signaling may be reiteratively involved during habenular differentiation cascade and being active even before its known “late” role in dHb neuron specification. Indeed, be visualizing Wnt activity in the *tg(7xtcf-Xla.Siam:nlsmCherry)*^{ia5} line, we showed that dHb precursors are experiencing Wnt signaling activity even if very low prior to 36 hpf suggesting that pathway activity may be present before that crucial stage. Importantly, this intermediate “steady state” can be overcome if Wnt signaling is activated via inhibition of a core component of the destruction complex Gsk3β. This is in line with previous observation showing that even at these early stages, the Wnt transduction

machinery is present in dHb precursors and is ready to be activated by upcoming Wnt ligands. We further showed that low levels of Wnt signalling are required for proper differentiation of dHb precursors as premature activation via LiCl or BIO leads to delayed differentiation of habenular neurons as assessed via the *Et(-1.0otpa:mmGFP)*^{hd1} transgene and the HuC/D staining at 48h. We found that the most robust delay is achieved while pathway activation is triggered in between 24hpf and 26hpf suggesting that during this time the majority of dHb precursors may experience a transition toward their neuronal commitment and that low levels of Wnt signaling would permit these cells to exit the precursor stage. Wnt signaling has already been implicated in the generation and maintenance of neuronal progenitor pools. Previous work from Kuan and collaborators (Kuan et al., 2015) showed that in *wingless* mutant (wls) where Wnt signaling is likely down-regulated, the size of the habenular precursor population marked by *dbx1b and cxcr4b* are markedly reduced. Also, in the embryonic hypothalamus Wnt up-regulation or Down-regulation result respectively in an increase or a decrease in the size of the neuronal progenitor pool (Wang et al., 2012). In the developing habenulae, Wnt signalling seems to be active in very few precursors before 36hpf, this level of activity could be therefore required for multipotent progenitors to enter and subsequently exit the precursor stage as excessive activation and suppression of the pathway has been proved to impair further development into their neuronal lineages.

4.2 The parapineal signal may suppresses Wnt signaling on Hb neuron at the time of their delayed differentiation

Habenular neurons are generated during two different waves of neurogenesis. During the first differentiation wave, occurring mainly on the left side, local alleviation of Wnt signalling via the parapineal enables post mitotic neurons to acquire the dHbl character (Concha et al., 2003, Gamse et al., 2003, Gamse et al., 2005, Hüsken et al., 2014). During the second wave, active Wnt signaling in dHb precursors biases them to become dHbm neurons. We showed that premature activation of Wnt signalling likely impairs Hb progenitors progression toward their neuronal fate. As a consequence, the overall neurogenesis in the habenulae is delayed, the first

differentiation wave passes and neurons are generated during the second wave and consequently acquire characteristics typical of dHbm neurons. However, even if we observe a clear bias toward the dHbm character, the expression of dHbl markers is never completely abolished. One possible explanation is that even if neurogenesis is delayed, some dHb precursor could still differentiate under the influence of the parpapineal and in this way acquire the dHbl character. Several evidences support this hypothesis: Fistly, it is likely that the transient drug treatments do not have a strong Wnt activation effect onto all cells and that the wif1 morpholino will generate a wif1 hypomorphic scenario rather than a loss of wif1. Secondly, in both LiCl treated embryos and wif1 morphants, the parapineal migrates normally showing no direct treatment influence. Also, while premature LiCl or BIO mediated Wnt activation causes a delay in habenular neuron differentiation, parapineal cell ablation appears not to influence this process (Roussigne et al., 2009), Furthermore we did not observe any obvious l-r differences in the number of Wnt active habenular precursors in the absence of the parapineal in Wnt reporter carrying embryos (data not shown) showing that indeed parapineal migration and function is uncoupled to early events controlling precursors transition into neurons. Therefore, it remains likely that following premature activation of Wnt signaling the parapineal would still be active on post mitotic neurons and act to suppress Wnt signaling and promote the dHbl character, however only very few neurons would fall under its influence.

4.3 Premature activation of Wnt phenocopies Notch overexpression

Our results define a role for Wnt signalling in controlling the timing of neurogenesis in the habenulae, so that if the pathway is prematurely active, precursors differentiate later than would naturally occur. Interestingly, a very similar effect can be obtained via transient overexpression of the Notch signalling pathway, which is classically considered an inhibitor of neuronal differentiation (Aizawa et al., 2007). Indeed, Notch up regulation before 30 hpf via the *Tg(hsp70:gal4)kca4; Tg(UAS:myc-notch1a-intra)kca3* transgenic line results in the majority of dHb neurons to acquire the dHbm character on both sides of the brain (Aizawa et al., 2007). It is therefore conceivable that the Wnt and the Notch signaling pathways may interact during the early phases of Hb neurogenesis. For instance, is possible that Notch signaling is exerting its action downstream Wnt signaling, so that premature activation of Wnt would promote Notch expression in precursors and in this way

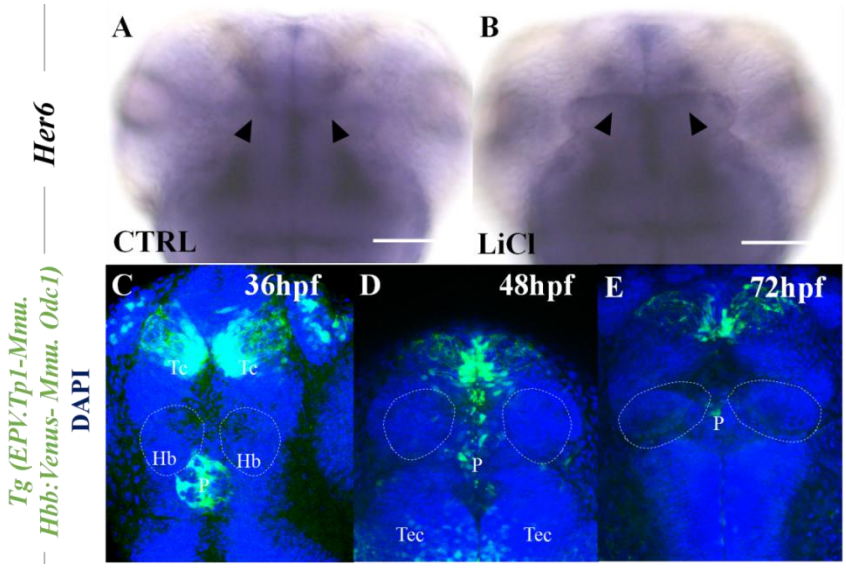

Figure 17: Investiganting the possible crosstalk between Wnt and Notch pathways

(A-E) Dorsal views with anterior to the top focused on the diencephalon at stages indicated. (A,B) *Her6* expression in the dyencephalon of 72 hpf larvae. LiCl treatment at 24-26 hpf result in a slight increase of Her6 expression across the ventricle posterior to the Habneulae (black arrow) (C-E) Expression of the *Tg (EPV.Tp1-Mmu. Hbb:Venus- Mmu. Odc1)*transgene cannot be detected in the Hb at any observed time-point. Hb, habenulae; Tec, tectum; P, pineal.

prevent their differentiation. In order to assess this intriguing possibility we performed a series of preliminary experiments to investigate whether high levels of Wnt signaling could trigger bilaterally prolonged Notch activity within the habenular precursor pool. The notch signaling effector *her6* is asymmetrically expressed within the developing habenulae during neuron differentiation, therefore has been suggested as likely factor controlling this process (Aizawa et al., 2007). At 36 hpf, *her6* expression is widespread in the anterior part of the dorsal diencephalon until 48 hpf. After this time-point, its expression is progressively reducing being confined to the peri-ventricular proliferative regions at 72hpf (data not shown). We found that early Wnt activation via LiCl do not markedly prolong or increase *her6* expression in the dorsal hypothalamus, we only observed a very slight increase in *her6* expression at 72hpf within the peri-ventricular region posterior to the Hb (Fig. 17A,B). However, it is unlikely that this effect was due to our early treatments. Is also possible that difference in *her6* could not be detected with our *in-situ* approach, as its expression appeared very strong also under control conditions. In order to overcome this problem we planned a more sensitive approach and used a Notch reporter line the *Tg (EPV.Tp1-Mmu. Hbb:Venus- Mmu. Odc1)*(Ninov et al., 2012) *(*In collaboration with Dr, Alessio Paolini, Potsdam University*)*. This line has been used to observe Notch dynamics *in-vivo* via expression of destabilized Venus (Ninov et al., 2012). Surprisingly, between 36 and 72 hpf transgene expression appeared very strong in the pineal, telencephalon and tectum but was absent in the presumptive habenulae beside very few peri-ventricular cells (Fig. 17C-E). We concluded that this reporter line is likely unable to recapitulate *her6* mediated Notch signalling in the habenulae. Therefore different approaches would be required for investigating the possible interplay between the different signaling pathways.

4.4 *Wif1* is strategically expressed within the presumptive habenulae

We found that the Wnt inhibitor *Wif1* is expressed in the presumptive habenulae during somitogenesis. This specific anatomical localization appears to be conserved amongst vertebrates as for instance in the mouse *wif1* expression can been strongly detected as early as E16.5 restricted to the medial habenular nucleus (MHb) (Yu-an Hu et al., 2008). Intriguingly, In the zebrafish, *wif1* expression displays a very peculiar expression time-course. The inhibitor is firstly detected in the habenulae around 20hpf at the time in which the precursor pool is likely to be established and appear to pick up around 24 hpf, the time at which LiCl mediated Wnt activation results in the most dramatic delay of differentiated dHb neurons. This is in line with previous observations suggesting that indeed around that stage most of dHb precursors may require strong protection against Wnt in order to exit the precursor stage. After 26 hpf, *wif1* expression start to progressively decrease until disappearing around 36 hpf, the time at which post mitotic dHb neurons start expressing Tcf7l2. However, the mechanism underlying such a fine regulation of *wif1* expression is still unclear. We proved that *wif1* expression can be modulated by Wnt signalling via a negative feedback mechanism. However, the expression of Wnt ligands like *wnt8b,* which is initially co-expressed with *wif1* in the epithalamus do not follow *wif1* expression pattern as its expression is persistent also after 36 hpf (Carl et al., 2007). Furthermore, in *axin1* mutants even if the level of *wif1* appear to be increased, the time course of *wif1* expression is not affected (data not shown) clearly denoting the involvement of an additional "Wnt- independent factor" in timely controlling *wif1* expression. One possibility is that this unknown factor may be downstream Wnt signaling and exclusively active in dHb precursors. Indeed, In between 26 and 36 hpf the pool of dHb precursor is progressively depleted in favor of differentiated neurons. It is therefore possible that while precursor differentiate, the expression of *wif1* is turned off so that the amount of Wif1 within the extra-cellular space is progressively reduced. Such a mechanism would ensure Hb precursors with strong protection from early Wnt signaling. However, this protection would be progressively alleviated as soon as differentiated neurons would become the predominant population, leading to an increase in the levels of Wnt signaling and the completion of the differentiation program.

4.5 Wif1 downregulation phenocopies premature Wnt induction

Early suppression of Wnt signaling is required for dHb precursors to differentiate into dHbl neurons. We provided evidences that wif1 is the likely molecule protecting dHb precursors from early Wnt ligands and therefore keeping the level of wnt pathway activity within the proper range. Our data show that Wif1 down-regulation phenocopies the pharmacological activation of Wnt signaling via LiCl or BIO. Indeed, in wif1 morphants, while dHb precursors seem to develop normally, dHb neuron differentiation is strongly delayed and the habenulae exhibit nearly all aspects a double right phenotype. However, in discordance with observation made on LiCl treated embryos, in wif1 morphants differentiated dHb neurons do not appear to be as strongly biased toward the dHbm charcter. A similar phenomenon has been described for *Tcf7l2* mutants in which symmetric innervation of the dIPN is accompanied by a complete loss of some of the dHbm markers like *kctd8* and *tag-1*, while others like *kctd12.2* and *brn3a* are still present in the habenulae (Husken et al 2014). Therefore it is likely that fate specification of dHb neurons is not a simple binary system, but different shades may exist depending on the molecular players affected at the time. For instance, it is possible that in LiCl treated embryos the majority of precursors are likely experiencing a strong and synchronous delay and very few amongst them will be influenced by the parapineal signal and acquire the dHbl character. Conversely, wif1 knockdown is likely leading to a lower but persistent activation of Wnt signaling over time until 36 hpf, the time at which *wif1* is no longer expressed. In this scenario only a fraction of dHb precursors would be progressively delayed over time and therefore more neurons would fall under the influence of the left sided parapineal signal. Still, these neurons apparently cannot fully complete their differentiation into dHbl neurons as in most cases dHb axons are exclusively innervating the ventral IPN. Notably, on about 10 hours have to pass in between the appearance of the first post mitotic dHb neuron (32hpf) and the onset of axonal branching toward the IPN (Beretta et al 2017). It is therefore possible that sustained high levels of Wnt signaling during this time could then trigger the expression of guidance molecules characteristic of dHbm neurons and guide Hb axons toward the vIPN.

4.6 Wif1 buffering of Wnt ligands shields developing dHb precursors from excessive Wnt signaling

Wif1 transcript levels are dependent on positive or negative oscillation in the activity of Wnt signaling. We did so by inhibiting Wnt via the secreted inhibitor Dkk1 which result in a marked reduction in *wif1* expression. The same result is obtained while Wnt is inhibited more downstream in the pathway, via the IWR drug which stabilizes Axin-1. We next demonstrated that *wif1* expression is dynamically increasing in response to increased levels of Wnt signalling and assessed this by bathing embryos in the two Wnt agonists LiCl and BIO. Interestingly, the intracellular nature of these treatments do not seem to enable the augmented extracellular wif1 to dampen excessive Wnt signaling. Indeed it is likely that as long as LiCl or BIO are bound to their target Gsk3β the Wnt pathway become insensitive to any sort of upstream signal. Intriguingly, when Wnt is induced at ligand level via *tg(hsp70l:Wnt8a-GFP)* we observed a very different scenario. Indeed, ectopic over-expression of the ligand lead to a dramatic expansion of the *wif1* expression domain which become extended toward the entire telencephalon. However, in contrary to what we observed in LiCl tratments, the habenulae develop normally and they axons correctly innervate and segregate into the dorsal and ventral parts of the IPN. The likely explanation is that in this case, the increase in Wif1 expression can completely neutralize the resulting excess of extracellular ligand. Notably, these results demonstrate that Wif1 possesses a very potent buffering capacity which makes it a prefectly dynamic shield to protect dHb precursors from early Wnt signaling. Furthermore, the increase in w*If1* expression observed in the telencephalon and other region were wif1 is naturally absent suggest that the Wif1 buffering system can be readily activated also in these region of brain. Therefore is conceivable that feedback inhibition from wif1 may be redundantly used in the developing embryo to protect cellular ensembles from deleterious oscillation of the Wnt signaling pathway.

4.7 Wif/Wnt negative feedback, a general mechanism to orchestrate neurogenesis in the brain

Following gastrulation, the developing vertebrate embryo is fine patterned into functional organs and domains. In the brain, this is mainly achieved through organizing centers, such as the midbrain-hindbrain boundary (MHB) and the mid-diencephalic organizer (MDO) or Zona Limitans Intrathalamica (ZLI) (Cavodeassi and Houart, 2012; Kiecker and Lumsden, 2012). The MDO is the responsible organizer for the patterning of anterior diencephalic structures like the thalamus and pre-thalamus and it does so by ensuring stable gradients of morphogens belonging to the Shh, Fgf and Wnt signaling pathways (Hagemann and Scholpp, 2012; Mattes et al., 2012). Interestingly, these ligands influence the behavior of MDO neighbouring cells in different ways across their gradient. While for instance the prethalamus anterior to the MDO develops only when Wnt activity is low, the thalamus posterior to the MDO requires Wnt signaling to develop (Mattes et al., 2012). Thus, Wnt ligands secreted from the MDO selectively activate Wnt signaling cascades in some MDO surrounding cells, while other cells must prevent this to happen. The perhaps most straightforward solution for such cells is to simply not express important Wnt signaling components like in the prethalamus (Hagemann and Scholpp, 2012; Jones and Rubenstein, 2004; Peukert et al., 2011; Quinlan et al., 2009; Shimogori et al., 2004) or to tightly control their temporal expression. Here we propose that as for the thalamus and pre-thalamus, patterning and neurogenesis of the dorsally positioned habenular nuclei is dependent on local modulation of the Wnt signalling pathway. We show that this is occurring via a two step mechanism dependent on the feedback activation of the Wif1 inhibitor. Our data are consistent with a model in which Wnt ligands originating from the MDO would locally trigger the expression of *wif1* in Hb precursor cells (Fig. 18A). Wif1 expression would then rise in response to the persisting Wnt gradient and dampen the level of the pathway to enable neuronal differentiation (Fig. 18B). After 36 hpf, *wif1* progressively shades away allowing TcF7l2 to mediate Wnt activity on post mitotic habenular neurons (Fig. 18D). In this way, the stable gradient of Wnt ligands is locally transduced in a specific temporal and spatial information capable of instructing dHb precursors toward their asymmetric neuronal destiny. Importantly, it is likely that beside Wnt signaling, other

morphogens may be involved in this process, as for instance the molecule responsible for shutting down *wif1* expression has yet to be found. Likely candidates could be Shh or Fgf pathways, which functions has already been linked to the patterning of diencephalic structures (Mattes et al., 2012; Halluin et al., 2016). Also, beside being expressed in the habenulae, *wif1* is expressed in other regions within the developing brain, always in combination with different Wnt ligands as for instance in the midbrain hindbrain boundary (MHB) or the hypothalamus (Thisse and Thisse, 2005; Thisse and Thisse, 2008). We found that *wif1* is transiently expressed in the presumptive IPN at the time in which dHb projection start the innervation of the midbrain nucleus. Consistently with our feedback model, induction of Wnt signaling during the same time profoundly affect IPN innervation, likely due to delayed

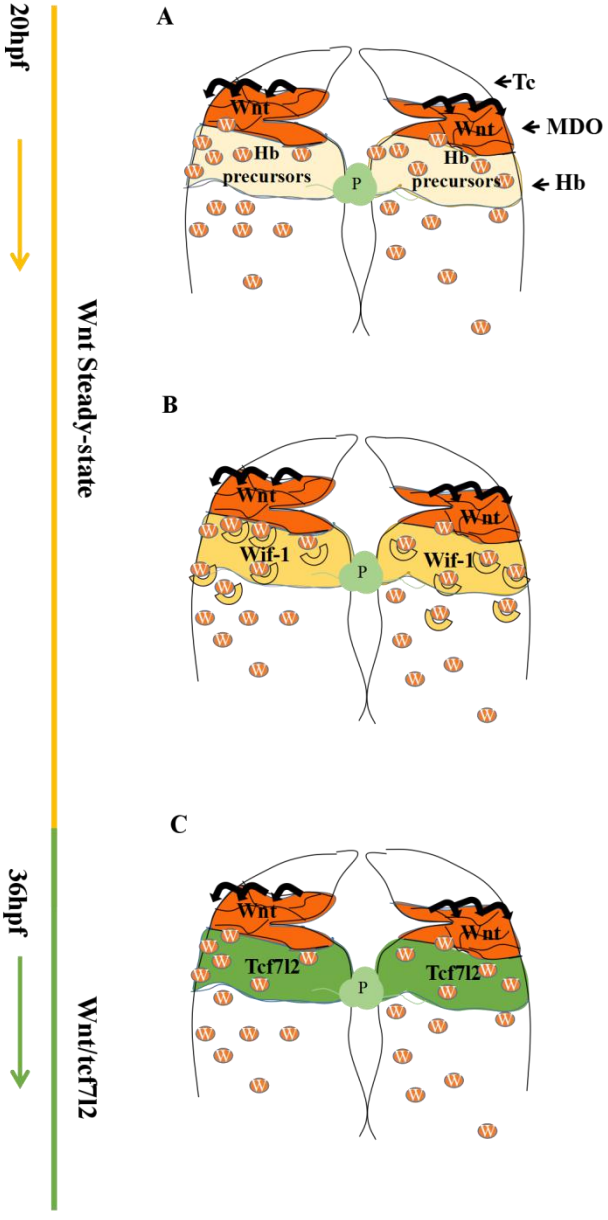

Figure 18: Wnt dependent induction of Wif1 enables neuronal differentiation in the Hb.

(A) Wnt ligands originating from the MDO trigger local expression of *wif1*

(B) Wif-1 is consequently being secreted in the extracellular space where it binds to Wnt ligands preventing Wnt activation in Hb precursors

(C) At 36 hpf Wif-1 expression is turned off due to a still unknown mechanism. Wnt ligands are now free to induce their Tcf7l2 dependent transcriptional program in post mitotic Hb neurons.Tc, telencephalon; MDO, mid-dyencephalic organizer; Hb, habenulae

neurogenesis within the IPN. These evidences suggest that indeed this model could be applied also to different regions in the brain highlighting a broader scenario in which the Wnt/wif1 negative feedback would serve as a mechanism for dynamically tuning neurogenesis across the different nuclei of the brain and synchronize their inter-connection at different time and space. The generation of genetic tools like a dynamic wif1 reporter transgenic line or a *wif1* knock out will likely help to clarify this point in the near future.

5. Experimental Procedures

5.1 Fish lines and maintenance

Zebrafish were maintained according to standard procedures (McNabb et al., 2012). For inhibition of pigmentation, embryos were incubated in 0.2 mM 1-phenyl-2 thiourea (PTU). AB wild type zebrafish and the following transgenic and mutant lines and were used: *Et(-1.0otpa:mmGFP)*^{hd1} (Beretta et al., 2017; Beretta et al., 2012), *tg(7xtcf-Xla.Siam:nlsmCherry)*^{ia5} (Moro et al., 2012), *tg(flh:GFP)*^{u711}*; tg(foxD3:GFP)*^{zf104} (Concha et al., 2003; Gilmour et al., 2002)*, tcf7l2*^{exl} (Muncan et al., 2007), *masterblind* (*mbl)*^{tm213} (Heisenberg et al., 2001), tg(*hsp70l:wnt8a-GFP)*^{w34} (Weidinger et al., 2005), and tg(*hsDkk1:GFP)* (Stoick-Cooper et al., 2007), *Tg(hsp70-brn3a:GFP)*^{rw0110b} (Aizawa et al., 2007), *Et(gata2a:EGFP)*^{pku588} (Hüsken et al., 2014). (Hüsken et al., 2014). Embryos were collected in E3 embryo medium and for in-situ hybridization and immunostaining proceducres embryos were decorionated with tweezers (No. 5 Dumont & Fils) and fixed at different developmental stages in 4.0% paraformaldehyde (PFA, Sigma) in PBS at room temperature for 3 hours or at 4° C over night**.** After fixation, the embryos were washed three times in 1X PBST rinsed two times for 5 minutes in 50% methanol in PBST and stored in 100% methanol (Sigma) at -20° C in 1.5 ml sterile tubes (Eppendorf).

E3 embryo medium:

- ✓ 5.0 mM NaCl (Sigma)
- ✓ 0.17 mM KCl (Sigma)
- ✓ 0.33 mM CaCl2 (Sigma)
- ✓ 0.33 mM MgSO4 (Sigma)
- ✓ 1.0% methylene blue (Sigma)

PBST

- ✓ 1XPBS
- ✓ 0.01% Tween 20, (Sigma)

Paraformaldehyde (4%) pH 7.0

- ✓ 1.33 M Paraformaldehyde (Sigma)
- ✓ 1X PBS (Sigma)

The pH was adjusted to 7 with NaOH (Sigma).

5.2 Generation of in-situ probes

For the synthesis of anti-sense probe used for the in-situ hybridizations procedure, the different plasmids were linearized with the respective restriction enzyme (see table below) using the following incubation parameters:

- ➢ 5U restriction enzyme
- ➢ 2µl enzyme buffer
- ➢ 5-10 ug Plasmid DNA
- ➢ Water up to 20 µl
- ➢ Incubate at 37 ℃

To check for optimal linearization, 2µl of linearized plasmid were loaded on a 1% agarose gel.

In situ probes	Enzyme for linearization	RNA polymerase	Reference
Wif-1	EcoRI-HF	T7	Hsieh et al., 1999)
kctd8	XhoI	Sp6	Gamse et al., 2005; Gamse et al., 2003
kctd12.1	EcoRI-HF	T7	Gamse et al., 2005; Gamse et al., 2003
kctd12.2	EcoRI-HF	T7	Gamse et al., 2005; Gamse et al., 2003
sst1	EcoRI-HF	Sp6	Thisse and Thisse, 2004
cxcr4b	Bam HI	T7	Roussigne et al., 2009

After digestion, linearized plasmids were purified using the QIAquick PCR Purification Kit (Quiagen) according to the manufacturer's instructions and purified plasmids were eluited in 30µl RNAse free water and the DNA concentration measured with the Nanodrop system. Subsequently eluted DNA was used for the following transcription reaction:

- 800ng-1.5µg linearized plasmid
- 2µl 10X RNA polymerase buffer
- 2.0 µl of DIG (digoxigenin) or FITC (fluorescein) labelling mix (Roche)
- 1µl of RNAse inhibitor (NEB)
- 2µl RNA polymerase (Sp6/T7)
- RNAse free water up to 20µl
- Incubate at 37° C for 3 hours

After the transcription the resulting RNA was cleaned up and concentrated using the RNeasy Cleanup Kit (Qiagen) according to the manufacturer's instructions. To ensure higher concentration levels, the in-situ probes were eluted in two steps with 30 ul of Milli-Q DNase/RNase free water. Each in-situ probe was checked by agarose gel electrophoresis and the concentration/purity was estimated using the Nanodrop system. The RNA probes were immediately used or stored at -20° C or at -80° C.

5.3 In-situ hybridization labeling

For the in-situ hybridization procedure the embryos were rehydrated in 50% methanol/PBST for 15 minutes on 1.5 ml sterilized eppendorf tubes and washed two times in PBST for 10 minutes. Embryos were then incubated in 10 µg/ml of proteinase K (Sigma) in PBST at room temperature for different times according to the developmental stages. No digestion was performed before somitogenesis stage while 15 minutes digestion was performed for embryos fixed at 24 hpf. For older embryos incubation was prolonged additional 15 minutes per day of development. After washing two times for 5 minutes in PBST, embryos were again fixed for 20min in 4% PFA at RT and again washed in PBST 5 times for 5 minutes each. After that, embryos were rinsed once in hybridization mix for 5 min before incubating them in hybridization mix for 2h at 65C° for pre-hybridization. In parallel, the in -situ probe was diluted in the hybridization mix and pre-incubated for 10 minutes at 65C°. After the pre-hybridization step, embryos were incubated with the hybridization mix containing probe overnight at 65-68 °C. The next day, embryos were washed several times at 65°C. First rinsed for 5 minutes in hybridization mix, than 30 minutes in 50% hybridization mix in 2X SSC and then washed two times in 0.2X SSC for 35 minutes. After that embryos were bathed in a solution of in 1:1 mixture of 0.1X SSC and MAB for 15 minutes and washed three times for 5 minutes in MAB. In order to prevent unspecific labeling, embryos were incubated in 2% blocking agent in MAB for 2hours. Afterwards, embryos were incubated overnight at 4 °C with a solution containing anti-digoxigenin-alkaline phosphatase (1:5000) or anti-fluorescein-isothiocyanate phosphatase (1:1000) antibodies diluted in MABL. The next day, embryos were washed from the antibody 4 times for 30 minutes in MAB at RT and equilibrated 3

times for 5 minutes in the staining buffer (DIG or FITC). In order to detect probe binding, embryos were transferred on a 24 well plate and incubated in the developmental substrate. For the DIG staining 1.0 ml of pre-mixed NBT/BCIP (Thermo Scientific) was used as developing substrate; for FITC reaction, the embryos were incubated at 28 °C with the Fast Red TR-Naphtol substrate (Sigma) in according to the manufacturer's instructions until the reaction was completed. Both colorimetric reactions were stopped by washing the embryos several times in PBST and the staining was fixed in 4% PFA for 1 hour. Stained samples were rinsed 3 times for 5 min in PBST at room temperature and stored in 75% glycerol in PBS at 4° C.

Hybridization mix (pH 6)

- 50% Formamide (Roth)
- ✓ 5X SSC
- ✓ 250 µg/ml Torula RNA (Sigma)
- ✓ 0.1% Tween 20 (Sigma)
- ✓ 50 µg Heparin (Applichem)

The pH was adjusted to 6.0 adding 1.0 M of citric acid.

20X SSC (pH 7)

- ✓ 0.30 M Sodium Citrate (Sigma)
- ✓ 3.0 M NaCl (Sigma)

MAB (pH 7.5)

- ✓ 100 mM Maleic Acid (Sigma)
- ✓ 150 mM NaCl (Sigma)
- ✓ 0.10% Tween 20 (Sigma)

MABL (pH 7.5)

- ✓ MAB + 2.0% Blocking Reagent (Roche)

Staining buffer (DIG)

- ✓ 5.0 ml 1.0 M Tris HCl (pH 9.0, 27° C; Sigma)
- ✓ 1.0 ml 5.0M NaCl (Sigma)
- ✓ 2.5 ml 1.0 M $MgCl_2$ (Sigma)
- ✓ 250 µl Tween 20 (Sigma)

The volume was adjusted to 50 ml with DD water.

Staining buffer (FITC)

- ✓ 0.10 M Tris HCl (pH 8.3, 27° C; Sigma)
- ✓ 0.10% Tween 20 (Sigma)

5.4 Antibody staining

Embryos were reihdrated digested and fixed as previously described (see section 5.3). After fixation in 4% PFA, embryos were washed at least 5 times for 5 minutes in PBSTr for 10 minutes and after the washing steps embryos were incubated in Incubation Buffer for 2 hours at RT on a shaking plate. This step is required for the blocking unspecific binding of the antibody. Next, the different primary antibodies (see table below) were diluted in 400-500 µl of Incubation Buffer and DAPI (1:1000 Thermo Scientific) was added for the nuclear staining. Samples were incubated overnight at 4° C on a shaking plate. Next day, the embryos were washed 5 times for 10 minutes with PBSTr and incubated in Incubation Buffer containing DAPI together with the secondary antibody (see table below) overnight at 4° C on a shaking plate. The samples were washed 4 times for 30 minutes with PBSTr immediately mounted and imaged by confocal laser scan microscopy.

PBSTr

- ✓ (X PBS + 1 % Triton-X-100 (Roth)

Incubation Buffer

- ✓ 1X PBS
- ✓ 0.8% Triton X-100 (Roth)
- ✓ 10% NGS (Normal Goat Serum; Invitrogen)
- ✓ 1.0% DMSO (Dimethyl Sulfoxide; Sigma)

Antibody	Diluition	Brand
Mouse anti-GFP	1:1000	Santa Cruz Biotechnology
Mouse anti-human TCF3,4	1:200	Sigma Aldrich
Mouse anti- HuC/D antibody	1:100	Invitrogen
Goat anti-mouse Alexa Fluor 488	1:250	Invitrogen
Goat anti-chicken Alexa Fluor 488	1:250	Invitrogen
Donkey anti-mouse Alexa Fluor 564	1:250	Invitrogen

5.5 Double fluorescence immuno-in-situ labellings

In order to perform double fluorescence immuno in-situ labelings, embryos were hybridized with the specific in-situ probe (see section 5.3) and before proceeding for the immunostaining (see section 5.4) embryos were fixed at room temperature for maximum 20 minutes and washed 3 times with PBST on a shaking plate (Macdonald et al., 1994; Shanmugalingam et al., 2000 and Carl et al., 2007).

5.6 Heat Shock and Drug Treatments

To manipulate Wnt signaling we used IWR (Sigma) as pharmacological antagonist and BIO ((2'Z,3'E)-6-Bromo-indirubin-3'oxime, Sigma) or LiCl (AppliChem) as pharmacological agonist. Experiments were performed by incubating dechorionated embryos either in IWR containing solutions (0.1 mM in E3 embryo medium/1% DMSO, Sigma) starting from 22 hpf for 3h or in BIO containing solution (10 uM in E3 embryo medium/0.15% DMSO), starting from 22hpf for 3h or 6h. Control groups were treated with 1% and 0.15% DMSO respectively. For LiCl treatments, various stages of embryos were exposed to 0.3 M LiCl in E3 embryo medium for 30 minutes at 28°C. Afterwards, embryos were washed repeatedly with E3 embryo medium and allowed to develop at 28°C. Heat shock experiments were performed as follows: tg*(*hsp70l:Wnt8a-GFP) and tg(hsDkk1:GFP) embryos were incubated for 45 min at 37°C starting from 22hpf. Transgenic embryos were identified by fluorescence and heat-shocked wild-type siblings were used as control.

5.7 Cell Counting and statistical analyses

To count dHb neurons we used anti-HuC/D immunostaining in combination with nuclear DAPI staining. 50 um confocal Z-stacks were acquired by using the pineal and epithalamic morphology as a landmark. Left and right HuC/D positive cells were counted using the software Fiji (NHI). To count Wnt-active cells in *tg(7xtcf-Xla.Siam:nlsmCherry); tg(flh:GFP); tg(foxD3:GFP)* transgenic embryos, 50 µm confocal Z-stacks were acquired in the developing dHb region. 20 µm Z-stacks (upper-limit defined by the uppermost pineal cell) were extracted from the raw data and mCherry positive cells were counted using the software Fiji (NHI). Equal orientation of the different embryos was ensured by comparing the morphology of the ventricle. Data are presented as means ± SD. The significance of differences between groups was investigated by Student's *t*-test (two tail, GraphPad software), and the following levels of significance used $*P < 0.05$; $**P < 0.02$; $***P < 0.001$.

5.8 Microscopy and Image Manipulation

For transmitted light pictures, larvae were mounted in glycerol and imaged using differential interference contrast optics (Leica CTR6000; 20× and 40× objectives). For fluorescence confocal microscopy, embryos were mounted in 1% low-melt agarose in glass-bottom dishes (MatTek or LabTek). Embryos were imaged by using A TCS SP5 MP (Leica) inverse laser scanning microscope, equipped with a pulsed IR laser for multi-photon excitation (Mai Tai HP, Spectra Physics) and two external filter-based detectors for multi-photon detection. Images were acquired with a 40× water objective (NA 1.1, Leica) and each Z-stack was acquired with a 1 µM interval. Stack analysis, Maximum Intensity Projections (MIPs), cropping and 2D-views were performed using the software Fiji.

5.9 Morpholino and mRNA injections

To knock down Wif1 function, established morpholino oligonucleotides for *Wif1* (Yin et al., 2012) were dissolved in water to a final working concentration of 1 mM. 1nl MO solution was injected into one cell stage embryos. Embryos were subsequently fixed at the different stages and processed for *in-situ* hybridization or antibody labeling. For in-vivo nuclei labeling, H2B-PSmOrange mRNA was trascribed and injected as follows: H2B-PSmOrange plasmid was linearized using the NotI restriction enzyme (NEB) and trascribed using the mMESSAGE mMACHINE® sp6 Kit (Ambion) at 37° C for 3 hours. After linearization the DNA was digested with 1.0 U of DNase I endonuclease (Fermentas) at 37° C for 10 minutes. Finally, the mRNA was cleaned up using the RNeasy Cleanup kit (Quiagen) and 200pg of H2B-PSmOrange mRNA were injected into one cell stage embryos.

5.10 Tcf7l2 mutants genotyping

Identification of *tcf7l2*$^{-/+}$ adults (Muncan et al., 2007) was performed by genotyping as follows: putative adult carriers were anesthetized in 0.04% tricain (Sigma) and fin clipping was performed. Namely, a small portion of the fin tissue was exported with a scalpel or a tweezers and inserted in a sterile eppendorf tube with 150µl of GNT-K buffer containing 100 µg/ml of proteinase K (Sigma) on ice. The adult fish were kept separately in mouse tanks and sorted according to the result of each genotyping. For Genomic DNA extraction, the excised tissue was incubated at 56° C for 4 hours. DUring incubation, each tube was vortexed and shortly spun down for 3-4 times. After incubation, the proteinase K was inactivated at 95° C for 10 minutes. The extracted DNA was stored at -20° C.

GNT-K buffer

- ✓ 10 mM Tris/HCl (pH 8, Sigma)
- ✓ 1mM EDTA (Sigma)
- ✓ 0,3% Tween (Sigma)
- ✓ 0,3% Glycerol (Sigma)

Tcf7l2 mutants carry a point mutation at the level of the first exon of the *Tcf7l2* gene which destroys the recognition sequence for the BsajI restriction enzyme (NEB). Therefore the genomic locus flanking the BsajI was amplified using the following primers:

Primer Forward:
5'- AAAATGCCGCAGCTGAAC -3'
Primer Reverse:
5'- CAACAACACGGTGCATCG -3'

PCR conditions (Taq DNA Polymerase kit, Quiagen)

Reagent	Amount
5x Taq Polymerase Buffer	5 µl
Q solution	10 µl
5mM MgCl2	5 µl
Primer forward	1 µl
Primer reverse	1 µl
10mM dNTPs Mix	1 µl
Quiagen Taq DNA Polymerase	1 µl
Purified genomic DNA	5 µl
H2O	Up to 50 µl

PCR program:

95° C 2 min
95° C 30 sec
63° C 30 sec
72° C 30 sec
go to step 2, repeat the cycle 30 times
72° C 5 min
4.0° C forever

The resulting amplicons were digested with the BsajI restriction enzyme (New England Biolab, NEB) under the following conditions:

- 16 µl PCR product
- 10X Cut Smart Buffer (NEB)
- 2µl BsajI
- Incubate at 60° C, 4 hours/overnight

Digested DNA was loaded on a 2% agarose gel.

5.11 Generation of a *wif1*$^{-/-}$ line by CRISPR/Cas9 genome editing

5.11.1 Designing of the gWifE2 and gWifE4 gRNAs

In order to generate gRNAs capable of inducing high efficiency DSBs on the *wif1* genomic locus, optimal target sequences were designed using the online gRNA predictor CCtop (Stemmer et al., 2015). This predictor provides gRNAs targeting sequences in the form of a forward and reverse 15-23 bp oligos, which can be subsequently annealed and cloned into the gRNA vector pDR274 (Hwang et al., 2013; Addgene #42250) for T7 mediated *in-vitro* trascription (Hwang et al., 2013; Stemmer et al., 2015). The Wnt binding domain (WIF) is represented by the first 4 exons of the *wif1* gene (Hsieh et al., 1999). Therefore the first 450 nucleotides of the *wif1* CDS were blasted within the CCtop online predictor. Among the output sequences, two of them were chosen due to poor off-target potential *gWifE2 (*GCCAGGTGAAGTTGACGTGA), targeting the 2nd exon and *gWifE4 (*AGCATTTGAGGTGACCATCC) targeting the 4th exon of the *wif1* gene.

Oligos specific for the 2nd exon (*gWifE2)*

Fw: TAgGCCAGGTGAAGTTGACGTGA

Rw: AAACTCACGTCAACTTCACCTGG

Oligos specific for the 4th exon (*gWifE4)*

Fw: TAggAGCATTTGAGGTGACCATCC

Rw: AAACGGATGGTCACCTCAAATGCT

5.11.2 Oligos annealing and phosphorylation

-Each oligo pair was annealed as follows:

- 6.3 µl Fw oligo (0.6 nmoles)
- 6.3 µl Rw oligo (0.6 nmoles)
- Water up to 75 µl

Briefly vortex, spin and incubate for 10 min at 95°C. Immediately transfer samples into a pre- heated bath at 85°C and turn the bath off so that the progressive lowering of the temperature will ensure proper annealing of the oligo pairs. Leave the reaction overnight.

Phosphorylation of the annealed oligos

- 6µl of annealed oligos
- 1µl DNA T4 ligase buffer (NEB)
- 1µl T4 polynucleotide kinase (NEB)
- Water up to 10 µl
- Incubate for 1hour at 37°C

Linearization and purification of the pDR274 vector

- 4-6 µg of pDR274
- 1µl of BsaI (NEB)
- 2µl of 10X CutSmart buffer (NEB)
- Water up to 20 µl
- Incubate overnight at 37°C
- Next day add 1µl of CIP and incubate for additional 90 min

Digested vector was loaded in 1% agarose gel and purified using the Gel Extraction Kit (Quiagen).

5.11.3 Ligation of the annealed oligos in the pDR274 vector

- 5µl of phosporylated oligos
- 10 ng of digested pDR274 vector.
- 1 µl of T4 ligase buffer (NEB)
- 1 µl of T4 ligase (NEB)
- Water up to 10µl
- Incubate overnight at 16°C.

Next day, bacterial transformation was performed as follows: competent TOP10 E-coli were defrosted in ice and the total ligation volume (10µl) was pipetted into the vial. The solution was then incubated for 30 min in ice. Readily after the incubation bacteria were transferred at 42°C for 30 sec in a pre-warmed thermoblock and than again in ice for 5 min. Next, 250µl of SOC medium were added to the solution and incubated at 37°C for 1hour at 300rpm. After this step, the entire solution was spread on LB agar plate and incubated overnight at 37°C. The next day, single colonies were picked and transferred in 5 ml LB containing Kanamicyn and incubated overnight at 37°C at 180 rpm. Finally bacteria were pelleted at 6000g for 15 min at 4°C and plasmid DNA was extracted and purified using the Plasmid miniprep kit (Quiagen).

LB-kanamycin agar plate

- ✓ Mix 40 g of LB agar
- ✓ 1g of agar
- ✓ Water up to 1L
- ✓ Autoclave the mixture
- ✓ Add 1 ml of 50 mg/ml kanamycin stock solution
  pour it into 40 10-cm Petri dishes.

LB-kanamycin medium

- ✓ 25 g of LB broth (Roth)
- ✓ Water up to 1L
- ✓ Autoclave the mixture

- ✓ Add 1 ml of 50 mg/ml kanamycin stock solution

In order to screen for positive clones, plasmid DNA was digested with the BsaI restriction enzyme, indeed positive integration of annealed oligos result in the destruction of the BsaI site on the pDR274

- 500ng/1µg plasmid DNA
- 2µl CutSmart buffer (NEB)
- 1µl BsaI (NEB)
- Water up to 20 µl
- Incubate overnight at 37°C

Digested plasmid was loaded on a 1% agarose gel. Gel electrophoresis resulted resulted in two different plasmid patterns: Supercoiled plasmid = positive for integration. Linearized =Negative for integration. Positive samples were sequenced with the M13 primer which ensures optimal coverage of the cloning site.

5.11.4 Trascription of the gRNAs and Cas9 mRNA

In order to transcribe the two different gRNAs, plasmid DNA was digested under the following conditions:

- 5µg of plasmid DNA
- 2µl CutSmart Buffer 10X (NEB)
- 1µl DraI (NEB)
- Water up to 20µl
- Incubate overnight at 37°C

Digested plasmid was purified using the DNA Cleanup Kit (Quiagen) and 1µg of eluted DNA was transcribed using the mMESSAGE mMACHINE T7 kit (Thermo Fisher Scientific). Finally, the resulting RNA purified with the RNACleanup kit (Quiagen) and RNA samples were stored at -80C for later injections.

To generate Cas9 mRNA, the Cas9 expression plasmid (Auer et al., 2014) was linearized using the BbsI enzyme:

- 5µg Plasmid DNA
- 2µl CutSmart Buffer (NEB)
- 1µl BbsI(NEB)
- Water up to 20ul
- Incubate at 37°C overnight

Once digested, the DNA was purified using the QIAquick PCR Purification Kit (Quiagen) and elute in a final volume of 15ul. Next 2µg of linearized plasmid were transcribed using the mMessage mMachine T7 Ultra kit (thermofisher) for 3 hours at 37°C. and at the end of the incubation, residual DNA was degraded by adding 1µl of turbo DNAse (thermofisher) and incubated for 10 minutes at 37°C. Finally, the RNA was purified via the following steps:

- Add 30 µl of the lithium chloride precipitation solution (provided in the mMessage mMachine T7 Ultra kit kit)
- Incubate the samples at −20 °C for 30 min
- Centrifuge the samples at 4 °C for 15 min at 14,000g and discard the supernatant
- Wash the pellet with 1 ml of 70% ethanol in H2O
- Centrifuge the mixture for 10 min at 14,000g
- Remove the supernatant
- Air-dry the pellet until it becomes transparent
- Resuspend the pellet in 60 µl of nuclease-free water
- Incubate the resuspended RNA sample at 65 °C for 10 min to dissolve the RNA
- Measure the RNA concentration using a spectrophotometer.
- Store Cas9 mRNA at −80 °C.

5.11.5 gRNAs injection and cleavage efficiency

One cell stage embryos were injected with 1nl of the following mix:

250ng gRNA
2.5µg Cas9 mRNA
Water up to 10µl

Injected embryos were either allowed to grow under standard condition or collected at 3dpf for DNA extraction and testing of gRNAs cleavage efficiency. Genomic DNA was extracted from freshly injected embryos, and both the putative gRNA cutting site amplified with MiSeq specific primer tags (Gagnon et al., 2014). The Illumina MiSeq technology enables single molecule sequencing and provide an overview of the entire range of Cas9 mediated modifications occurring within a specific locus (Gagnon et al., 2014). Briefly, pool of 10 embryos at 3dpf were transferred on single eppendorf tubes, the E3 medium removed and substituted with 180 µl GNT buffer and 20 µl of Proteinase K was added. Samples were incubated at 55°C for 2 hours to enable Proteinase K digestion. Proteinase K was then inactivated by incubating the embryos at 95°C for 10 min. After DNA extraction, amplification of the desired locus was performed using the following primers and conditions:

MiSeqWif1Fw1:
TCGTCGGCAGCGTCAGATGTGTATAAGAGACAGAATAGTCTCTGAGGGGA
AAATGG

MiSeqWif1Rw1:
GTCTCGTGGGCTCGGAGATGTGTATAAGAGACAGCTGTTTATGATGTATAT
ACTTTTTAAGCC

MiSeqWif1Fw2:
TCGTCGGCAGCGTCAGATGTGTATAAGAGACAGCATACATACTGAGATCT
GTGGCATG

MiSeqWif1Rw2
GTCTCGTGGGCTCGGAGATGTGTATAAGAGACAGCAATCAAAAAAGTTTG
GACAGCAG

PCR mix

Reagent	Amount
5µl 10X High Fidelity PCR buffer (Invitrogen)	5 µl
1µl 10mM dNTPs mix	1 µl
2µl 50mM $MgSO_4$	5 µl
1µl MiSeqWif1Fw1 or MiSeqWif1Fw2	1 µl
1µl MiSeqWif1Rw1 or MiSeqWif1Rw2	1 µl
2µl Genomic DNA	1 µl
0.2µl Platinum Taq DNA Polymerase High Fidelity (Invitrogen)	1 µl
Water	Up to 50µl

PCR program

1: 94°C 60sec
2: 94°C 15sec
3: 56°C 30sec
4: 68°C 30sec
Go to step 2, repeat the cycle 35 times
5: 4°C forever

Amplicons were loaded on a 2.5% agarose gel and purified using the Gel purification kit Quiagen according to manifacturer instruction. Next, eluted samples were diluted to 20ng/µl and sent to Dr. Ana Faro (Steve WIlson lab, UCL, London) for further processing with the MiSeq sequencer (Gagnon et al., 2014). Finally sequences were analyzed with the Geneious software (Biomatters).

5.11.6 Identification of mutant alleles

Once injected embryos reached adulthood, putative FO carrier were crossed with WT fish and from each cross 10 single embryos were transferred on a 96 well plate together with 18ul GNT-K buffer and 2 ul of proteinase K. Embryos were than incubated at 55 °C for 4 hours and the PK inactivated at 95 °C for 10 min. Afterwards, putative cutting site were PCR amplified and processed as described in section 5.11.4-5.11.5)

6. References

Aizawa, H., Bianco, I.H., Hamaoka, T., Miyashita, T., Uemura, O., Concha, M.L., Russell, C., Wilson, S.W., and Okamoto, H. (2005). Laterotopic representation of left-right information onto the dorso-ventral axis of a zebrafish midbrain target nucleus. Curr. Biol. 15, 238–243.

Aizawa, H., Goto, M., Sato, T., Okamoto, H. (2007). Temporally regulated asymmetric neurogenesis causes left-right difference in the zebrafish habenular structures. Dev. Cell 12, 87–98.

Amo, R.., Aizawa, H., Takahoko, M., Kobayashi, M., Takahashi, R., Aoki, T., Okamoto H. (2010). Identification of the zebrafish ventral habenula as a homolog of the mammalian lateral habenula. J. Neurosci. 30, 1566–157410.1523/ JNEUROSCI.3690-09.2010

Auer., TO, Duroure, K., Concordet, JP., Del Bene, F.(2014). CRISPR/Cas9-mediated conversion of eGFP- into Gal4-transgenic lines in zebrafish. Nat Protoc. 9(12):2823-40. doi: 10.1038/nprot.2014.187.

Benabid, AL., Jeaugey, L. (1989). Cells of the rat lateral habenula respond to high-threshold somatosensory inputs. Neurosci Lett. 1989 Jan 30;96(3):289-94.

Beretta, CA., Dross, N., Bankhead, P., Carl, M. (2013). The ventral habenulae of zebrafish develop in prosomere 2 dependent on Tcf7l2 function. Neural Dev. 8:19. doi: 10.1186/1749-8104-8-19.

Boulos, LJ., Darcq, E., Kieffer, BL. (2016). Translating the Habenula-From Rodents to Humans.Biol Psychiatry. 81(4):296-305. doi: 10.1016/ j.biopsych.2016.06.003.

Beretta, CA., Dross, N., Guiterrez-Triana, JA., Ryu, S., Carl, M. (2012).Habenula circuit development: past, present, and future. Front. Neurosci. 6, 51.

Beretta, CA., Dross, N., Guglielmi, L., Bankhead, P., Soulika, M., Gutierrez-Triana JA., Paolini, A., Poggi, L., Falk, J., Ryu, S., Kapsimali, M., Engel, U., Carl M. (2007). Early Commissural Diencephalic Neurons Control Habenular Axon Extension and Targeting. Curr Biol. 27(2):270-278. doi: 10.1016/j.cub.2016.11.038.

Bianco, IH., Carl, M., Russell, C., Clarke, JD., Wilson, SW.(2008). Brain asymmetry is encoded at the level of axon terminal morphology. Neural Dev,.3:9. doi: 10.1186/1749-8104-3-9.

Bianco, IH. and Wilson, SW. (2009). The habenular nuclei: a conserved asymmetric relay station in the vertebrate brain. Phil. Trans. R. Soc. B Biol. Sci. 364, 1005–1020

Boerboom, D., White, LD., Dalle, S., Courty, J., Richards, JS. (2006). Dominant-stable beta-catenin expression causes cell fate alterations and Wnt signaling antagonist expression in a murine granulosa cell tumor model. Cancer Research. 66, 1964-1973

Caneparo, L., Huang, YL., Staudt, N., Tada, M., Ahrendt, R., Kazanskaya, O., Niehrs, C., Houart, C. (2007). Dickkopf-1 regulates gastrulation movements by coordinated modulation of Wnt/beta catenin and Wnt/PCP activities, through interaction with the Dally-like homolog Knypek. Genes Dev. 21(4):465-80.

Carl, M., Bianco, IH., Bajoghli., Aghaallaei, N., Czerny, T., Wilson, SW.(2007). Wnt/Axin1/beta-catenin signaling regulates asymmetric nodal activation, elaboration, and concordance of CNS asymmetries. Neuron.. 55(3):393-405

Cavodeassi, F. and Houart, C., (2012). Brain regionalization: of signaling centers and boundaries. Dev Neurobiol. 72, 218-233.

Chou, MY., Amo, R., Kinoshita, M., Cherng, BW., Shimazaki, H., Agetsuma, M., Shiraki, T., Aoki, T., Takahoko, M., Yamazaki, M., Higashijima, S., Okamoto, H. (2016). Social conflict resolution regulated by two dorsal habenular subregions in zebrafish. Science. 352(6281):87-90. doi: 10.1126/science.aac9508.

Concha, ML., Burdine, RD., Russell, C., Schier, AF., Wilson SW. (2000). A nodal signaling pathway regulates the laterality of neuroanatomical asymmetries in the zebrafishforebrain. Neuron. 28(2):399-409.

Concha, ML. And Wilson, SW. (2001). Asymmetry in the epithalamus of vertebrates. J Anat. 199(Pt 1-2):63-84.

Concha, ML., Russell, C., Regan, JC., Tawk, M., Sidi, S., Gilmour, DT., Kapsimali, M., Sumoy, L., Goldstone, K., Amaya, E., Kimelman, D., Nicolson, T., Gründer, S., Gomperts, M., Clarke, JDW., Wilson, SW. (2003). Local tissue interactions across the dorsal midline of the forebrain establish CNS laterality. Neuron. 39, 423-438.

Concha, ML., Bianco, IH., Wilson, SW. (2012). Encoding asymmetry within neural circuits. Nat Rev Neurosci,13(12):832-43. doi: 10.1038/nrn3371.

Corballis, M.C. (2012). Lateralization of the human brain. Prog. Brain Res. 195, 103–121.

Cowling, VH., D′Cruz, CM., Chodosh, LA., Cole, MD. (2007). c-Myc transforms human mammary epithelial cells through repression of the Wnt Inhibitors DKK1 and SFRP1. Molecular Cell Biology. 27, 5135-5146.

Crossley, P.H., Martinez, S. and Martin, G.R., 1996. Midbrain development induced by FGF8 in the chick embryo. Nature. 380, 66-68.

Dean, BJ., Erdogan, B., Gamse, JT., Wu, SY. (2014). Dbx1b defines the dorsal habenular progenitor domain in the zebrafish epithalamus. Neural Dev. doi: 10.1186/1749-8104-9-20.

deCarvalho, TN., Subedi, A., Rock, J., Harfe, BD., Thisse, C., Thisse, B., Halpern, ME., Hong, E. (2014). Neurotransmitter map of the asymmetric dorsal habenular nuclei of zebrafish. Genesis. 2014 Jun;52(6):636-55. doi: 10.1002/dvg.22785.

De Strooper, B. and Annaert, W. (2001). Where Notch and Wnt signaling meet. J Cell Biol. 2001 Feb 19;152(4):F17-20.

Diep, DB., Hoen, N., Backman, M., Machon, O., Krauss, S. (2004). Characterisation of the Wnt antagonists and their response to conditionally activated Wnt signalling in the developing mouse forebrain. Brain Res Dev Brain Res. 153, 261-270

Dharmaretnam, M. and Rogers, LJ. (2005). Hemispheric specialization and dual processing in strongly versus weakly lateralized chicks. Behav. Brain Res. 162, 62–70.

Dreosti, E., Vendrell Llopis, N., Carl, M., Yaksi, E., and Wilson, SW. (2014). Left-right asymmetry is required for the habenulae to respond to both visual and olfactory stimuli. Curr. Biol. 24, 440–445. doi: 10.1016/j.cub.2014.01.016

Duboc, V., Dufourcq, P., Blader, P., and Roussigne, M. (2015). Asymmetry of the Brain: Development and Implications. Annu. Rev. Genet. 49, 647–672.

Facchin, L., Duboué, ER., Halpern, ME. (2015). Disruption of Epithalamic Left-Right Asymmetry Increases Anxiety in Zebrafish. J Neurosci. 35(48):15847-59. doi: 10.1523/JNEUROSCI.2593-15.2015.

Güntürkün, O., Ocklenburg, S. (2017). Ontogenesis of Lateralization. Neuron. 2017 Apr 19;94(2):249-263. doi: 10.1016/j.neuron.2017.02.045.

Grimshaw, GM., and Carmel, D. (2014). An asymmetric inhibition model of hemispheric differences in emotional processing. Front. Psychol. 5, 489.

Gamse, JT., Thisse, C., Thisse, B., Halpern, ME. (2003). The parapineal mediates left-right asymmetry in the zebrafish diencephalon. Development. Mar;130(6):1059-68.

Gamse, J.T., Kuan, Y.S., Macurak, M., Bro ¨ samle, C., Thisse, B., Thisse, C., Halpern, M.E. (2005). Directional asymmetry of the zebrafish epithalamus guides dorsoventral innervation of the midbrain target. Development 132, 4869–4881.

Garric L, Ronsin B, Roussigné M, Booton S, Gamse JT, Dufourcq P, Blader P. (2014). Pitx2c ensures habenular asymmetry by restricting parapineal cell number. Development. Apr;141(7):1572-9. doi: 10.1242/dev.100305.

Gayoso, JÁ., Castro, A., Anadón, R., and Manso, MJ. (2011). Differential bulbar and extrabulbar projections of diverse olfactory receptor neuron populations in the adult zebrafish (*Danio rerio*). J. Comp. Neurol. 519, 247–276. doi: 10.1002/cne.22518

Gagnon, JA., Valen, E., Thyme, SB., Huang, P., Akhmetova, L., Pauli, A., Montague TG., Zimmerman, S., Richter, C., Schier, AF. (2014). Efficient mutagenesis by Cas9 protein-mediated oligonucleotide insertion and large-scale assessment of single-guide RNAs. PLoS One. 9(5):e98186. doi: 10.1371/journal.pone.0098186. eCollection 2014

Gilmour, DT., Maischein, HM., Nüsslein-Volhard, C. (2002). Migration and function of a glial subtype in the vertebrate peripheral nervous system. Neuron. 34, 577-588.

Hagemann, AIH. and Scholpp, S. (2012). The tale of the three brothers – Shh, Wnt, and Fgf during development of the thalamus. Frontiers in Neuroscience. 6:76.

Halluin, C., Madelaine, R., Naye, F., Peers, B., Roussigné, M., Blader P. (2016). Habenular Neurogenesis in Zebrafish Is Regulated by a Hedgehog, Pax6 Proneural Gene Cascade. PLoS One. 11(7):e0158210. doi: 10.1371/journal.pone.0158210.

Halpern, ME., Liang, JO., Gamse, JT. (2003) Leaning to the left: laterality in the zebrafish forebrain.Trends Neurosci. 26(6):308-13.

Heisenberg, CP., Houart, C., Take-uchi, M., Rauch, GJ., Young, N., Coutinho, P., Masai, I., Caneparo, L., Concha, ML., Geisler, R., Dale, TC., Wilson, SW., Stemple, D.L. (2001). A mutation in the Gsk3-binding domain of zebrafish Masterblind/Axin1 leads to a fate transformation of telencephalon and eyes to diencephalon. Genes & Development. 15, 1427-1434.

Herkenham, M. and Nauta WJH. (1977). Afferent connections of the habenular nuclei in the rat. A horseradish peroxidase study, with a note on the fiber-of-passage problem. J. Comp. Neurol. 173, 123–14610.1002/cne.90173010

Hirokawa N, Tanaka Y, Okada Y, Takeda S. (2006). Nodal flow and the generation of left-right asymmetry. Cell. 125(1):33-45.

Hisano, Y., Sakuma, T., Nakade, S., Ohga, R., Ota, S., Okamoto, H., Yamamoto T., Kawahara, A. (2005). .Precise in-frame integration of exogenous DNA mediated by CRISPR/Cas9 system in zebrafish. Sci Rep. 5:8841. doi: 10.1038/srep08841.

Hobert, O., Johnston, R.J., Jr., and Chang, S. (2002). Left-right asymmetry in the nervous system: the Caenorhabditis elegans model. Nat. Rev. Neurosci. 3, 629–640

Hong, E., Santhakumar, K., Akitake, C. A., Ahn, SJ., Thisse, C., Thisse, B., Wyart C., Mangin JM., Halpern, ME. (2013). Cholinergic left-right asymmetry in the habenulo-interpeduncular pathway. Proc. Natl. Acad. Sci. U S A 110, 21171–21176. doi: 10.1073/pnas.1319566110

Hsieh, JC., Kodjabachian, L., Rebbert, ML., Rattner, A., Smallwood, PM., Harryman Samos, C., Nusse, R. and Nathans, J. (1999). A new secreted protein that binds to Wnt proteins and inhibits their activites. Nature. 398, 431-436.

Huang, P., Xiong, F., Megason, SG., Schier, AF. (2012). Attenuation of Notch and Hedgehog signaling is required for fate specification in the spinal cord. PLoS Genet. 8(6):e1002762. doi: 10.1371/journal.pgen.1002762.

Hüsken, U., Stickney, HL., Gestri, G., Bianco, IH., Faro, A., Young, R.M., Roussigne, M., Hawkins, TA., Beretta, CA., Brinkmann, I.., Paolini. A., Jacinto, R., Albadri, S., Dreosti, E., Tsalavouta, M., Schwarz, Q., Cavodeassi, F., Barth, A.K., Wen, L., Zhang, B., Blader, P., Yaksi, E., Poggi, L., Zigman, M., Lin, S., Wilson, SW., Carl, M. (2014). Tcf7l2 is required for left-right asymmetric differentiation of habenular neurons. Current Biology. 24, 2217-2227.

Hutsler, J., and Galuske, RAW. (2003). Hemispheric asymmetries in cerebral cortical networks. Trends Neurosci. 26, 429–435

Hu, YA., Gu, X., Liu, J., Yang, Y., Yan, Y., Zhao, C. (2008). Expression pattern of Wnt inhibitor factor 1(Wif1) during the development in mouse CNS.Gene Expr Patterns. 8(7-8):515-22. doi: 10.1016/j.gep.2008.06.001.

Hwang, WY., Fu, Y., Reyon, D., Maeder, ML., Tsai, SQ., Sander, JD., Peterson, RT., Yeh, JR., Joung, JK. (2013). Efficient genome editing in zebrafish using a CRISPR-Cas system. Nat Biotechnol. 31(3):227-9. doi: 10.1038/nbt.2501.

Jetti, SK., Vendrell-Llopis, N., Yaksi, E. (2014). Spontaneous activity governs olfactory representations in spatially organized habenular microcircuits. Curr. Biol. 24, 434–439. doi: 10.1016/j.cub.2014.01.015

Jones, EG. and Rubenstein, JL. (2004). Expression of regulatory genes dur-ing differentiation of thalamic nuclei in mouse and monkey. J Comp Neurol. 477, 55-80.

Kansara, M., Tsang, M., Kodjabachian, L., Sims, N.A., Trivett, MK., Ehrich, M., Dobrovic, A., Slavin, J., Choong, PF., Simmons, PJ., Dawid, IB., Thomas, D.M., (2009). Wnt inhibitory factor 1 is epigenetically silenced in human osteosarcoma, and targeted disruption accelerates osteosarcomagenesis in mice. J Clin Invest. 119, 837-851.

Karlebach, G., and Francks, C. (2015). Lateralization of gene expression in human language cortex. Cortex 67, 30–36

Kawano, Y. and Kypta, R. (2003). Secreted antagonists of the Wnt signalling pathway. J Cell Sci. 116, 2627–2634.

Kiecker, C. and Lumsden, A. (2012). The role of organizers in patterning the nervous system. Annu Rev Neurosci. 35, 347-367.

Koshiba, M., Kikuchi, T., Yohda, M., Nakamura, S. (2002). Inversion of the anatomical lateralization of chick thalamofugal visual pathway by light experience. Neurosci. Lett. 318, 113–116.

Koshiba, M., Nakamura, S., Deng, C., Rogers, LJ. (2003). Light-dependent development of asymmetry in the ipsilateral and contralateral thalamofugal visual projections of the chick. Neurosci. Lett. 336, 81–84.

Krishnan, S., Mathuru, AS., Kibat, C., Rahman, M., Lupton, C. E., Stewart, J., Claridge-Chang, A., Yen, SC., Jesuthasan, S. (2014). The right dorsal habenula limits attraction to an odor in zebrafish. Curr. Biol. 24, 1167–1175. doi: 10.1016/j.cub.2014.03.073

Kuan, YS., Roberson, S., Akitake, CM., Fortuno, L., Gamse, J., Moens, C., Halpern, ME.(2015). Distinct requirements for Wntless in habenular development. Dev Bio, .406(2):117-128. doi: 10.1016/j.ydbio.2015.06.006.

Lee, M.J., Kim, E.J., Li, L., Jung, HS. (2015). Roles of Wnt inhibitory factor 1 during tooth morphogenesis. Cell Tissue Res. 362, 61-68.

Licchesi, JD., Van Neste, L., Tiwari, VK., Cope, L., Lin, X., Baylin, SB., Herman, JG. (2010). Transcriptional regulation of Wnt inhibitory factor-1 by Miz-1/c-Myc. Oncogene. 29, 5923-5934.

Louvi, A. and Artavanis-Tsakonas, (2006). Notch signalling in vertebrate neural development. Nat. Rev. Neurosci. 7: 93–102

MacDonald, BT., Tamai, K., He, X. (2009). Wnt/beta-catenin signaling: components, mechanisms, and diseases. Dev Cell. 17(1):9-26. doi: 10.1016/j.devcel.2009.06.016.

Mattes, B., Weber, S., Peres, J., Chen, Q., Davidson, G., Houart, C., Scholpp, S. (2012). Wnt3 and Wnt3a are required for induction of the mid-diencephalic organizer in the caudal forebrain Neural Development. 7:12.

McNabb, A., Scott, K., Von Ochsenstein, E., Seufert, K., Carl, M. (2012). Don't be afraid to set up your fish facility. Zebrafish. 9, 120-125.

Miyasaka, N., Morimoto, K.., Tsubokawa, T., Higashijima, S.I., Okamoto, H., Yoshihara, Y. (2009). From the olfactory bulb to higher brain centers: genetic visualization of secondary olfactory pathways in zebrafish. J. Neurosci. 29, 4756–4767. doi: 10.1523/JNEUROSCI.0118-09.2009

Morgane, PJ., Galler, JR., Mokler, DJ. (2005). A review of systems and networks of the limbic forebrain/ limbic midbrain. Prog. Neurobiol. 75, 143–16010.1016/j.pneurobio.2005.01.00

Moro, E., Ozhan-Kizil, G., Mongera, A., Beis, D., Wierzbicki, C., Young, R.M., Bournele, D., Domenichini, A., Valdivia, L.E., Lum, L., Chen, C., Amatruda, J.F., Tiso, N., Weidinger, G., Argenton, F.(2012). In vivo Wnt signaling tracing through a transgenic biosensor fish reveals novel activity domains. Developmental Biology. 366, 327-340.

Muncan, V., Faro, A., Haramis, APG., Hurlstone, AFL., Wienholds, E., van Es, J., Korving, J., Begthel, H., Zivkovic, D. and Clevers, H. (20079. T-cell factor 4 (Tcf7l2) maintains proliferative compartments in zebrafish intestine. EMBO reports. 8, ///966-973./

Ortiz, C.O., Faumont, S., Takayama, J., Ahmed, H.K., Goldsmith, A.D., Pocock, R., McCormick, K.E., Kunimoto, H., Iino, Y., Lockery, S., and Hobert, O. (2009). Lateralized gustatory behavior of C. elegans is controlled by specific receptor-type guanylyl cyclases. Curr. Biol. 19, 996–1004.

Peukert, D., Weber, S., Lumsden, A., Scholpp, S. (2011). Lhx2 and Lhx9 Determine Neuronal Differentiation and Compartition in the Caudal Forebrain by Regulating Wnt Signaling. PLOS Biology. 9(12): e1001218.

Picker, A., Brennan, C., Reifers, F., Böhli, H., Holder, N., Brand, M. (1999). Requirement for zebrafish acerebellar/FGF8 in midbrain polarization, mapping and confinement of the retinotectal projection. Development. 126, 2967-2978.

Quinlan, R., Graf, M., Mason, I., Lumsden, A. and Kiecker, C. (2009). Complex and dynamic patterns of Wnt pathway gene expression in the developing chick forebrain. Neural Development. 4:35.

Ramachandran, I., Thavathiru, E., Ramalingam, S., Natarajan, G., Mills, WK., Benbrook, DM., Zuna, R., Lightfoot, S., Reis, A., Anant, S. and Queimado, L. (2012). Wnt inhibitory factor 1 induces apoptosis and inhibits cervical cancer growth, invasion and angiogenesis in vivo. Oncogene. 31, 2725-2737.

Rebagliati, MR., Toyama, R., Fricke, C., Haffter, P., Dawid, IB. (1998). Zebrafish nodal-related genes are implicated in axial patterning and establishing left-right asymmetry. Dev Biol. 199(2):261-72.

Regan, JC., Concha, ML., Roussigne, M., Russell, C., Wilson, SW.(2009). An Fgf8-dependent bistable cell migratory event establishes CNS asymmetry. Neuron. 61(1):27-34. doi: 10.1016/j.neuron.2008.11.030.

Rilling, JK., Glasser, MF., Jbabdi, S., Andersson. J., Preus,s TM. (2011). Continuity, divergence, and the evolution of brain language pathways. Front Evol Neurosci.doi: 10.3389/fnevo.2011.00011. eCollection 2011.

Roberson, S., Halpern, MC. (2017). Convergence of signaling pathways underlying habenular formation and axonal outgrowth in zebrafish. Development, 144: 2652-2662; doi: 10.1242/dev.147751

Rogers, L.J. (1990). Light input and the reversal of functional lateralization in the chicken brain. Behav. Brain Res. 38, 211–221.

Rogers, LJ. Deng, C.(1999). Light experience and lateralization of the two visual pathways in the chick. Behav. Brain Res. 98, 277–287.

Rogers, L. J. (2000).Evolution of hemispheric specialization: advantages and disadvantages. Brain Lang. 73, 236–253

Rogers, LJ., Andrew, RJ., Johnston, AN. (2007). Light experience and the development of behavioural lateralization in chicks: III. Learning to distinguish pebbles from grains. Behav. Brain Res. 177, 61–69

Roussigné, M., Bianco, IH., Wilson, SW., Blader, P. (2009). Nodal signalling imposes left-right asymmetry upon neurogenesis in the habenular nuclei. Development, 136: 1549-1557; doi: 10.1242/dev.034793

Sampath, K., Rubinstein, AL., Cheng, AM., Liang, JO., Fekany, K., Solnica-Krezel L, Korzh, V., Halpern, ME, Wright, CV. (1998), Induction of the zebrafish ventral brain and floorplate requires cyclops/nodal signalling. Nature. 395(6698):185-9.

Schenker, NM., Hopkins, WD., Spocter, MA., Garrison, AR., Stimpson, CD., Erwin, JM., Hof, PR., Sherwood, CC. (2010). Broca's area homologue in chimpanzees (Pan troglodytes): probabilistic mapping, asymmetry, and comparison to humans. Cereb Cortex. :730-42. doi: 10.1093/cercor/bhp138. Epub 2009 Jul 20.

Schier, AF. (2003). Nodal signaling in vertebrate development. Annu Rev Cell Dev Biol. 2003;19:589-621.

Scholpp, S., Foucher, I., Staudt, N., Peukert, D., Lumsden, A., Houart, C. (2007). Otx1l, Otx2 and Irx1b establish and position the ZLI in the diencephalon. Development, 134: 3167-3176; doi: 10.1242/dev.001461

Shimogori, T., Vansant, J., Paik, E., Grove, EA. (2004). Members of the Wnt, Fz, and Frp gene families expressed in postnatal mouse cere-bral cortex. J Comp Neurol. 473, 496-510.

Stemmer, M., Thumberger, T., Del Sol Keyer, M., Wittbrodt, J., Mateo, JL. (2005). CCTop: An Intuitive, Flexible and Reliable CRISPR/Cas9 Target Prediction Tool. PLoS One. -0(4):e0124633. doi: 10.1371/journal.pone.0124633. eCollection 2015.

Stoick-Cooper, CL., Weidinger, G., Riehle, K.J., Hubbert, C., Major, MB., Fausto, N., Moon, R.T. (2007). Distinct Wnt signaling pathways have opposing roles in appendage regeneration. Development. 134, 467-478.

Sutherland, R.J. (1982). The dorsal diencephalic conduction system: A review of the anatomy and functions of the habenular complex. Neurosci. Biobehav. Rev. 6, 1-13.

Tervaniemi, M., and Hugdahl, K. (2003). Lateralization of auditory-cortex functions. Brain Res. Brain Res. Rev. 43, 231–246.

Thisse, C. and Thisse, B. (2005). High Throughput Expression Analysis of ZF-Models Consortium Clones. ZFIN Direct Data Submission.

Thisse, C., and Thisse, B. (2008). High-resolution in situ hybridization to whole-mount zebrafish embryos. Nature Protocols. 3, 59-69.

Toga, AW, and Thompson, PM.(2003). Mapping brain asymmetry. Nature Reviews Neuroscience 4, doi:10.1038/nrn1009

Turner, KJ., Bracewell, TG., and Hawkins, TA. (2014). Anatomical dissection of zebrafish brain development. Methods Molecular Biology. 1082, 197-214.

Vaes, B.L., Dechering, KJ., van Someren, EP., Hendriks, JM., van de Ven, CJ., Feijen, A., Mummery, CL., Reinders, MJ., Olijve, W., van Zoelen, EJ. and Steegenga, WT. (2005). Microarray analysis reveals expression regulation of Wnt antagonists in differentiating osteoblasts. Bone. 36, 803-811.

Vogel, JJ., Bowers, CA.,Vogel, DS. (2003). Cerebral lateralization of spatial abilities: a meta-analysis. Brain Cogn. 52, 197–204.

Wang, X., Kopinke, D., Lin, J., McPherson, AD., Duncan, RN., Otsuna, H., Moro, E., Hoshijima, K., Grunwald, DJ., Argenton, F., Chien, CB., Murtaugh, LC., Dorsky RI. (2012).Wnt signaling regulates postembryonic hypothalamic progenitor differentiation. Dev Cell. 23(3):624-36. doi: 10.1016/j.devcel.2012.07.012.

Weidinger, G., Thorpe, CJ., Wuennenberg-Stapleton, K., Ngai, J. and Moon, RT. (2005). The Sp1-Related Transcription Factors sp5 and sp5-like Act Downstream of Wnt/beta-Catenin Signaling in Mesoderm and Neuroectoderm Patterning. Curr Biol. 15, 489-500.

Wes, P.D., and Bargmann, C.I. (2001). C. elegans odour discrimination requires asymmetric diversity in olfactory neurons. Nature 410, 698–701

Wissmann, C., Wild, PJ., Kaiser, S., Roepcke, S., Stoehr, R., Woenckhaus, M., Kristiansen, G., Hsieh, JC., Hofstaedter, F., Hartmann, A., Knuechel, R., Rosenthal, A. and Pilarsky, C. (2003). WIF1, a component of the Wnt pathway, is down-regulated in prostate, breast, lung, and bladder cancer. J Pathol. 201.

Xu, B., Chen, C., Chen, H., Zheng, SG., Bringas, PJ., Xu, M., Zhou, X., Chen, D., Umans, L., Zwijsen, A. and Shi, W. (2011). Smad1 and its target gene Wif1 coordinate BMP and Wnt signaling activities to regulate fetal lung development. Development. 138, 925-935.

Young, R., Reyes, A., Allende, M. (2002). Expression and splice variant analysis of the zebrafish tcf4 transcription factor. Mech. Dev. 117, 269-273.

Yin, A., Korzh, V., Gong, Z., (2012). Perturbation of zebrafish swimbladder development by enhancing Wnt signaling in Wif1 morphants. BBA Molecular Cell Research. 1832, 236-244.

Zhang, BB., Yao, YY., Zhang, HF., Kawakami, K., Du, JL. (2017). Left Habenula Mediates Light-Preference Behavior in Zebrafish via an Asymmetrical Visual Pathway. Neuron. 93(4):914-928.e4. doi: 10.1016/j.neuron.2017.01.011.

Zirn, B., Samans, B., Wittmann, S., Pietsch, T., Leuschner, I., Graf, N., Gessler, M. (2006). Target genes of the WNT/beta-catenin pathway in Wilms tumors. Genes Chromosomes Cancer. 45, 565-574.

7.Appendix

7.1 Supplementary tables

Table S1 related to figure 7: LiCl treatments of Et(-1.0otpa:mmGFP) embryos

Hpf	WT	Reduced or absent GFP expression in the dHb (48hpf)	n
22	16(82%)	3(18%)	19
24	0	80(100%)	80
26	3(20%)	12(80%)	15
28	18(77%)	6(17%)	24
30	20(90%)	2(10%)	22

Table S2 related to figure 8-9: Effect of LiCl treatments on dHb neuron markers

Marker	WT	Reduced	Absent	n
HuC/D (48hpf)	1(11%)	8(89%)	0	9
Cxcr4b (48hpf)	28(93%)	2(7%)	0	30
kctd12.1(72hpf)	11(20%)	24(43%)	20(37%)	55
Et(gata2a:EGFP) (72hpf)	8 (20%)	18(45%)	14(35%)	40
kctd8 (72hpf)	10(20%)	32(67%)	6(13%)	48
Tg(hsp70-brn3a:GFP) (72hpf)	23(85%)	4(15%)	0	27
Kctd12.2 (72hpf)	39(63%)	15(24%)	8(13%)	62

Table S3 related to Figure 8, 12 and 14: Premature Wnt activation results in vIPN innervation

Treatment	WT	Only ventral	n
LiCl	4 (13%)	27(87%)	31
Wif1 MO	5 (19%)	21(81%)	26
BIO	1(25%)	3 (75%)	4
tg(hsp70l:wnt8a-GFP) @22hpf	9(100%)	0	9

Table S4 related to figure11,12: Wif1 knock down phenocopies LiCl treatments

Marker	WT	Reduced	Absent	n
Et(-1.0otpa:mmGFP) (48hpf)	13 (29%)	5 (12%)	25 (59%)	43
HuC/D (48hpf)	0	5 (100%)	0	5
Cxcr4b (48hpf)	17 (94%)	1(5%)	0	18
kctd12.1(72hpf)	26(37%)	30 (42%)	13(19%)	71
Et(gata2a:EGFP) (72hpf)	7 (23%)	7(23%)	17 (54%)	31
kctd8 (72hpf)	21(46%)	16(38%)	9 (18%)	46
Tg(hsp70-brn3a:GFP) (72hpf)	6 (60%)	4 (40%)	0	10
Kctd12.2 (72hpf)	22 (58%)	14 (37%)	2 (5%)	38

Table S5 related to figure 13: *Wif1* expression depends on Wnt signaling

Marker	WT	Reduced	Increased	n
tg(hsp701:wnt8a-GFP) @22hpf	0	0	46 (100%)	46
LiCl@22hpf	10 (30%)	0	23 (70%)	33
BIO@22hpf	4 (44%)	0	5(56%)	9
Axin1$^{-/-}$	8 (32%)	0	17(68%)	25
IWR@22hpf	8 (24%)	36(76%)	0	44
tg(hsDkk1:GFP) @22hpf	2 (6%)	31 (94%)	0	33
Tcf7l2 (whole incross clutches)	135(100%)	0	0	135

Table S6 related to figure 14: effect of tg(hsp70l:wnt8a-GFP)@22hpf on dHb markers

Marker	WT	Reduced	Increased	n
kctd12.1	18(86%)	2 (9.5%)	1 (4.5%)	21
Kctd8	8 (89%)	1 (11%)	0	9

7.2 List of figures

7.3 Abbreviations

A	adenosine
ace	acerebellar
APC	adenomatous polyposis coli
BIO	(2'Z,3'E)-6-Bromoindirubin-3′-oxime
bp	basepairs
C	cytosine
cxcr4b	C-X-C chemokine receptorr 4b
cyc	cyclops
d	dorsal
DNA	deoxyribonucleic acid
DDC	dorsal diencephalic conduction system
dHb	dorsal habenula
dHbl	lateral dorsal habenula
dHbm	medial dorsal habenula
DIG	digoxigenin-alkaline
DMSO	dimethylsulfoxide
dNTP	deoxyribonucleosidtriphosphate
Dpf	days post fertilization
E. coli	Escherichia coli
EDTA	ethylendiamintetraacetate
eGFP	enhanced green fluorescent protein
EmT	eminentia thalami
FGF	fibroblast growth factor
FITC	fluorescein-isothiocyanate
flh	floating-head
fw	foward
FR	fasciculus retroflexus
G	guanine
GFP	green fluorescent protein
GSK3	Glykogen Synthase Kinase 3
Hb	habenulae

hpf	hours post fertilization
hsp	heatshock promoter
IPN	interpeduncular nucleus
IWR	(1,3,3a,4,7,7a-Hexahydro-1,3-dioxo-4,7-methano-2H-isoindol-2-yl)-N-8-quinolinyl-Benzamid
kb	kilobase
KCTD	potassium channel tetramization domain
L	left
lHb	lateral habenula
LPM	lateral plate mesoderm
M	molarity
mbl	masterblind
mHb	medial habenula
Mib	mindbomb
min	minute
Mo	morpholino
MR	median raphe
oep	one-eyed pinhead
P	probability/P
PBS	phosphate buffered saline
PCP	planar cell polarity
PCR	polymerase chain reaction
PFA	paraformaldehyde
pitx2	paired-loke homeodomain transcription factor2
pp	parapineal
PTU	phenyl-2-thiourea
R	right
Rw	reverse
RNA	RNA ribonucleic acid
RT	room temperature
SD	standard deviation

sec	seconds
spw	southpaw
T	thymine
Taq	Thermophilus aquaticus
Tc	telencephalon
Tcf	T-cell specific transcripton factor
Tec	tectum
tg	transgene
Tris	Tris (hydroxymethyl)aminomethan
v	ventral
VTA	ventral tegmental area
Wif1	Wnt inhibitor factor 1
WT	wildtype

Aknowledgements

During the last three years I had the opportunity to meet extremely bright scientists which allowed me to grow both as scientist and as a human. Without them I would have never learn as much and managed to end my P.hD. thesis. First I would like to thank my mentor PD. Dr. Matthias Carl, for his knowledge, patience and example. He has been an incredible guide and helped me both on the scientific and human side in the moments I needed the most. I consider myself particularly lucky for having had the opportunity to met him. I am very thankful for the support I have got from the members of my TAC committee, Prof. Joachim Wittbrodt and Dr. Ruiz de Almodóvar. Their impressive knowledge has been inspiring me and helping me critically analyze my data and interpret their biological significance. I would like to thank Prof. Steve Wilson for hosting me in his lab and for giving me the opportunity to share my data with all the lab members. Especially Dr. Ana Faro and Dr. Gareth Powell and our every-day brainstormings on Wnt-signaling, I would like to thank all my present and former colleagues at the CBTM, especially Dr. Alessio Paolini and Dr. Carlo Beretta for their advises and the time spent both on the bench and outside from the lab as well as all the people in the ZBIO team. Leaving aside the scientific environment, I am very thankful to my family, for all the unconditioned support and motivation they have been giving to me. Also, during these years I had the opportunity to build solid and valuable relationships with very special people. First my girlfriend and colleague, Margot Maurer, who inspired me and supported me every day allowing me to overcome obstacles that seemed insurmontable. A special thanks to Sara Laiouar, with which I spent nearly all my days in the CBTM for being so kind with me and for being there whenever I needed. Finally I would like to thank all my closest friends and colleagues, Vladimir Riabov, Georg Sedlmeier, Nitin Patil, Mohammed Abba, Dajana Tanasic as they made my stay in the CBTM unforgettable.